SURFACE PROCESSES OF THE GREENLAND ICE SHEET UNDER A WARMING CLIMATE

Konrad Steffen, Thomas Phillips, Liam Colgan, Daniel McGrath

University of Colorado at Boulder
Cooperative Institute for Research in Environmental Sciences
Campus Box 216, Boulder CO 80309

NASA Grant NNX08AT85G

Progress Report
to
National Aeronautics and Space Administration

April 2010

CREVASSES IN LOWER PART OF JAKOBSHAVN ISBRAE FILLED WITH WATER

Table of Content

1. Field Expedition 2009

1.1 Logistic Summary

Date	Location	Work
April 2009		
20	Scotia-SFJ	Team members (Steffen, Colgan, McGrath) w/C-130
24	SFJ-Swiss Camp	Cargo load
24	Swiss Camp - NASA U	AWS download, extend tower
26	SFJ – NASA SE	AWS download, upgrade instruments
26	NASA SW - Saddle	AWS download, upgrade instruments
27	SFJ – Swiss Camp.	Put in (Steffen, Colgan, McGrath, Zwally)
27	SC – Up50 – CP1 – SC	AWS download, GPS download
28	SC (Swiss Camp)	AWS download
29	JAR1, JAR2	AWS download
May 2009		
3	SC	Corner reflectors placed for over flight
4	JAR1	Snow pit and AWS work
4	SC	Free Spirit Film team arrives
6	Moulin	GPS download, AWS re-drilling
11	JAR2	Re-drilling and upgrade
14	SC-SFJ	Swiss Camp pull-out
15	SFJ-SDome-SFJ	AWS download, upgrade instruments
16	SFJ-DyeII-SFJ	AWS download, upgrade instruments
17	SFJ-US	Team members Colgan, McGrath back to US
17	SFJ-Summit	Team Steffen and Schroff to Summit
18	Summit	AWS download, upgrade instruments
20	Summit	AWS upgrade
23	Summit	50 m tower upgrade
29	Summit-SFJ	Team Steffen and Schroff return to Kanger
30	SFJ-NEEM	Upgrade NEEM AWS, royal visit
31	NEEM-SFJ	Return from NEEM royal visist
June 2009		
1	SFJ-CPH	Steffen leaving via Copenhagen

1.2 Automatic Weather Station Maintenance

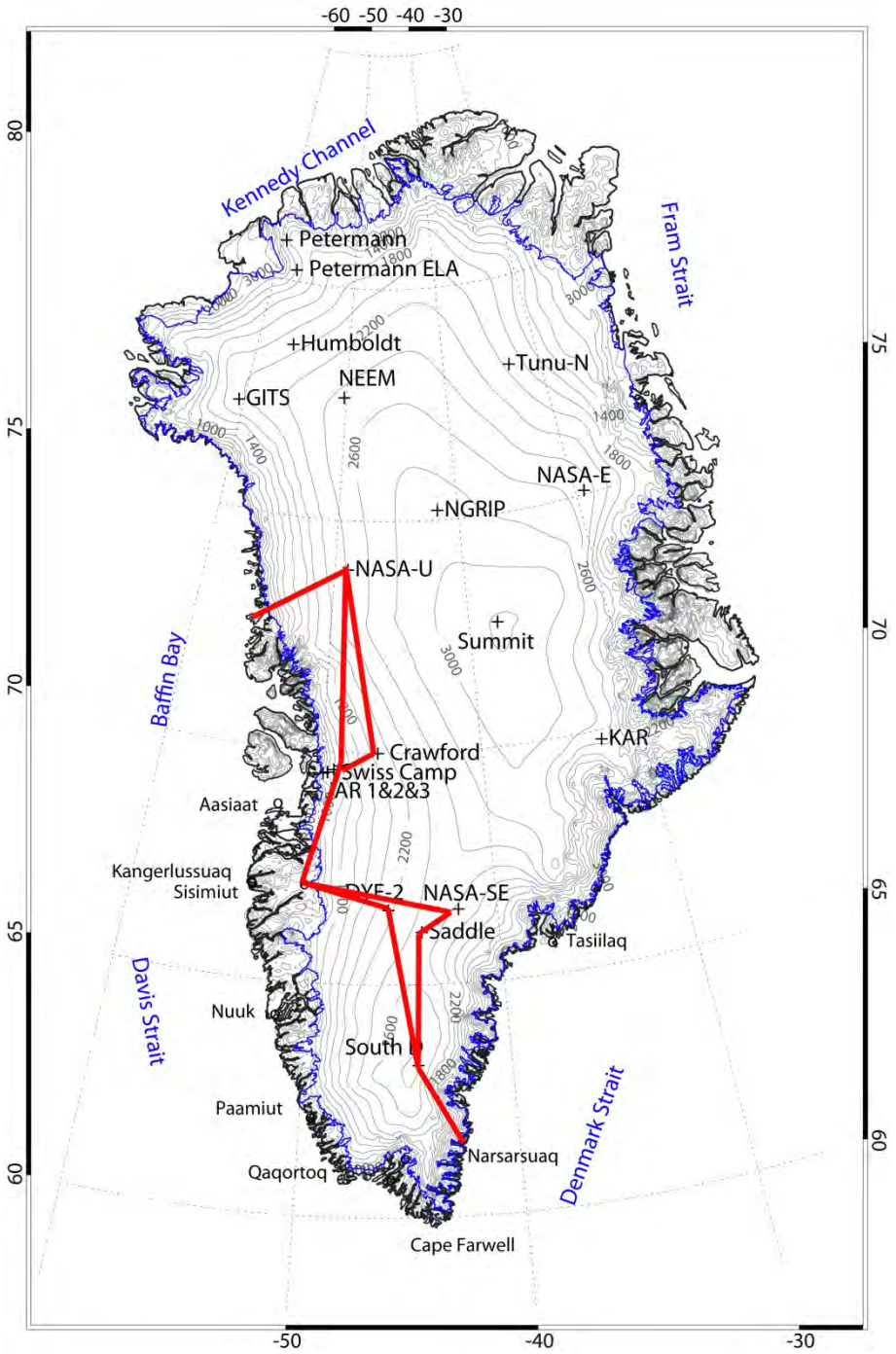

Figure 1.1: Greenland Climate Network (GC-Net) automatic weather stations as of summer 2009. The red arrows indicate the Twin Otter flight path for the AWS maintenance described in the logistic summary.

1.3 Personal

Name	Institution	Arr.	Dep.
AWS support, Swiss Camp research, Summit station			
Konrad Steffen	CU-Boulder	4/20	6/2
William Colgan	CU-Boulder	4/20	5/17
Dan McGrath	CU-Boulder	4/20	5/17
Jay Zwally	NASA-GSFC	4/26	5/11

2. Introduction

2.1 Overview

The GC-Net currently consists of 17 automatic weather stations and four smart stakes distributed over the entire Greenland ice sheet (Figure 1.1). Four stations are located along the crest of the ice sheet (2500 to 3200 m elevation range) in a north-south direction, Eight stations are located close to the 2000 m contour line (1830 m to 2500 m), and three stations are positioned in the ablation region (50 m to 800 m), and two stations are located at the equilibrium line altitude at the west coast and in the north.

The GC-Net was established in spring 1995 with the intention of monitoring climatological and glaciological parameters at various locations on the ice sheet over a time period to assess the climate and its variability. The first AWS was installed in 1990 at the Swiss Camp, followed by four AWS in 1995, four in 1996, five in 1997, another four in 1999, one in 2002 one in 2003, and the latest one at NEEM in support for the new deep ice core in 2006. Our objectives for the Greenland weather station (AWS) network are to measure daily, annual and interannual variability in accumulation rate, surface climatology and surface energy balance at selected locations on the ice sheet, and to measure near-surface snow density at the AWS locations for the assessment of snow densification, accumulation, and metamorphosis.

In addition to providing climatological and glaciological observations from the field, further application of the GC-Net data include: the study of the ice sheet melt extent (*Abdalati and Steffen*, 2001); estimates of the ice sheet sublimation rate (*Box and Steffen*, 2001); reconstruction of long-term air temperature time series (*Shuman at al.*, 2001), assessment of surface climate (*Steffen and Box*, 2001), and the interpretation of satellite-derived melt features of the ice sheet (*Nghiem et al.*, 2001). Potential applications for the use of the GC-Net data are: comparison of in-situ and satellite-derived surface parameters, operational weather forecast; validation of climate models; and logistic support for ice camps and Thule AFB.

2.2 GC-Net Users

The GC-Net data request from the beginning of 2009 to present (23 April 2010) register 184 individual user request (Table 2.1). The web interface allows us to capture the email and affiliation of all GC-Net users, including a short description of their use of the Greenland Climate data. The data request is processed on a UNIX 4-processor workstation and the data is transferred on a FTP site for direct downloading. We will continue to maintain the main portal for all GC-Net data distribution, the main raison being the frequent data reprocessing to increase data quality.

298	mzhang@notes.cc.sunysb.edu	minghua zhang	SUNY at stony Brook	Approved 01-20-09 @ 11:26 am		
299	fxsm@uaf.edu	Sebastian H. Mernild	IARC, University of Alaska Fairbanks	Approved 01-07-09 @ 6:42 am		
300	gregor.hillebrand@gmx.de	Gregor Hillebrand	univerity Kassel / Germany	Approved 01-08-09 @ 5:17 am		
303	rrniii@gmail.com	Ryan Neely	CIRES/ESRL	Approved 09-20-09 @ 2:59 pm		
304	xianweiw@uci.edu	xianwei wang	University of California- Irvine	Approved 01-28-09 @ 6:16 pm		
305	koni@seaice.colorado.edu	Koni	cu	Approved 01-15-09 @ 12:41 am		
306	robinson@pik-potsdam.de	Alexander Robinson	Potsdam Institute for Climate Impact Research	Approved 03-16-10 @ 9:30 am		
307	bhattacharya.21@osu.edu	Indrajit	the ohio state university	Approved 01-20-09 @ 11:32 am		
308	bjartnes@gmail.com	BjÃ¸rn Einar Bjartnes	.	Approved 01-23-09 @ 11:35 am		
309	rodtsimpson@yahoo.com	Rodney Simpson	Natural Resource Ecology Laboratory, Colorado State University	Approved 01-23-09 @ 11:37 am		
310	valerie.masson@cea.fr	Masson-Delmotte Valérie	LSCE Gif sur Yvette France	Approved 01-26-09 @ 6:29 pm		
311	claudia.monstein@hispeed.ch	Monstein Claudia		Approved 01-27-09 @ 9:25 am		
312	jburkhart@ucmerced.edu	John Burkhart	University of California Merced	Approved 10-01-09 @ 12:13 pm		
313	kasper.jakobsen@hotmail.com	Kasper Jakobsen	Technical University of Denmark	Approved 02-02-09 @ 5:42 am		
315	valerie.masson@cea.fr	Masson-Delmotte	LSCE Gif sur Yvette France	Approved 02-05-09 @ 1:37 am		
316	guisheng@umd.edu	sheng gui	university of maryland	Approved 02-10-09 @ 12:16 am		
317	michellekbozeman@gmail.com	Michelle Bozeman	Clark University	Approved 02-10-09 @ 4:19 pm		
318	guisheng@umd.edu	sheng gui	university of maryland	Approved 02-11-09 @ 12:04 am		
319	guisheng@umd.edu	sheng gui	university of maryland	Approved 02-11-09 @ 5:34 pm		

320	guisheng@umd.edu	sheng gui	university of maryland	Approved 02-16-09 @ 1:32 am		
322	guisheng@umd.edu	sheng gui	university of maryland	Approved 02-16-09 @ 2:41 pm		
323	katherine.pingree@umit.maine.edu	Katherine Pingree	University of Maine, Department of Earth Sciences	Approved 03-05-09 @ 4:28 pm		
324	bai@polarmet1.mps.ohio-state.edu	Lesheng Bai	Byrd Polar Research Center, The Ohio State University	Approved 02-27-09 @ 4:03 pm		
325	r.braithwaite@manchester.ac.uk	Roger Braithwaite	University of Manchester	Approved 03-05-09 @ 4:29 pm		
326	nicolle.britland@gmail.com	Nicolle Britland	University of Otago, Dunedin, New Zealand	Approved 04-08-09 @ 5:08 am		
327	michellekbozeman@gmail.com	Michelle Bozeman	Clark University	Approved 03-19-09 @ 10:29 pm		
328	robinson@pik-potsdam.de	Alex Robinson	PIK	Approved 03-22-09 @ 10:49 am		
329	schwander@climate.unibe.ch	Jakob Schwander	Climate and Environmental Physics, University of Bern	Approved 03-24-09 @ 8:53 pm		
330	ehanna@sheffield.ac.uk	Edward Hanna	University of Sheffield	Approved 03-26-09 @ 9:20 am		
331	rcrain@nsf.gov	Renee Crain	National Science Foundation and George Mason University	Approved 03-30-09 @ 12:10 pm		
332	pasteris@dri.edu	Dan Pasteris	Desert Research Institute, Reno, Nevada, USA	Approved 04-01-09 @ 6:09 pm		
333	konrad.steffen@colorado.edu	Koni	CU	Approved 04-02-09 @ 11:51 pm		
334	hjw38@cam.ac.uk	Humphrey Waddington	Scott Polar Research Institute, Cambridge	Approved 04-07-09 @ 9:09 am		
335	hanschr@gfy.ku.dk	Hans Christian Steen-Larsen	Centre for Ice and Climate, University of Copenhagen	Approved 04-07-09 @ 9:09 am		
336	JJAIMOE@MSN.COM	JULIE MILLER	UNIVERSITY OF UTAH	Approved 04-08-09 @ 5:08 am		
337	muto@colorado.edu	Atsuhiro Muto	NSIDC/CIRES	Approved 04-08-09 @ 6:37 pm		
338	muto@colorado.edu	Atsuhiro Muto	NSIDC/CIRES	Approved 04-12-09 @ 2:37 pm		
339	john.adler@colorado.edu	John Adler	CIRES	Approved 04-12-09 @ 2:35 pm		
340	rcrain@nsf.gov	Renee Crain	NSF, George Mason University	Approved 04-14-09 @ 10:43 pm		
341	rcrain@nsf.gov	Renee Crain		Approved 04-14-09 @ 10:51 pm		

342	rcrain@nsf.gov	Renee Crain		Approved 04-14-09 @ 10:52 pm	
343	rcrain@nsf.gov	Renee Crain	NSF, George Mason University	Approved 04-14-09 @ 10:53 pm	
344	rcrain@nsf.gov	Renee Crain	National Science Foundation and George Mason University	Approved 04-14-09 @ 10:55 pm	
345	rcrain@nsf.gov	Renee Crain	National Science Foundation and George Mason University	Approved 04-14-09 @ 10:56 pm	
346	rcrain@nsf.gov	Renee Crain	National Science Foundation and George Mason University	Approved 04-14-09 @ 10:57 pm	
347	rcrain@nsf.gov	Renee Crain	National Science Foundation and George Mason University	Approved 04-14-09 @ 10:58 pm	
348	rcrain@nsf.gov	Renee Crain	National Science Foundation and George Mason University	Approved 04-14-09 @ 11:04 pm	
349	rcrain@nsf.gov	Renee Crain	National Science Foundation and George Mason University	Approved 04-14-09 @ 11:05 pm	
350	rcrain@nsf.gov	Renee Crain	National Science Foundation and George Mason University	Approved 04-14-09 @ 11:08 pm	
351	zedlam@ku.edu	dave besson	University of Kansas, Dept. of Physics	Approved 04-25-09 @ 6:11 am	
352	david.docquier@student.ulg.ac.be	Docquier David	University of Liège	Approved 04-26-09 @ 7:45 pm	
353	cyr.derek@gmail.com	Derek Cyr	University at Albany	Approved 04-29-09 @ 4:41 pm	
355	venkats@colorado.edu	Ambika	CIRES	Approved 05-01-09 @ 8:51 am	
356	berdanie@rams.colostate.edu	Aaron	Colorado State University	Approved 05-07-09 @ 2:43 pm	
357	hjw38@cam.ac.uk	Humphrey Waddington	Scott Polar Research Institute	Approved 05-19-09 @ 7:37 pm	
358	florian.figwer@gmail.com	Figwer Florian	University Innsbruck	Approved 10-15-09 @ 3:37 am	
359	hjwaddington@googlemail.com	Humphrey Waddington	Scott Polar Research Institute	Approved 09-07-09 @ 5:27 pm	
360	jweber@unidata.ucar.edu	Jeff Weber	UCAR/NCAR	Approved 05-26-09 @ 1:42 pm	
361	daniel.west@umontana.edu	Dan West	University of Montana, Department of Geosciences	Approved 09-07-09 @ 5:28 pm	
362	daniel.west@umontana.edu	Dan West	University of Montana, Department of Geosciences	Approved 06-03-09 @ 2:28 pm	
363	ehanna@sheffield.ac.uk	Edward Hanna	University of Sheffield	Approved 06-05-09 @ 10:01 pm	

364	chaneyn@berkeley.edu	Nathaniel Chaney	REU UC Irvine	Approved 06-29-09 @ 2:17 pm		
365	john.adler@colorado.edu	John Adler	CIRES	Approved 06-30-09 @ 1:46 pm		
366	ctt@geus.dk	Charlotte Thomsen	GEUS	Approved 07-01-09 @ 1:20 pm		
367	john.adler@colorado.edu	John Adler	CIRES	Approved 07-07-09 @ 10:20 am		
368	wangzhs@bu.edu	Zhuosen Wang	Boston University	Approved 07-08-09 @ 10:28 am		
369	wuhongyi1008@163.com	Hongyi Wu	University of Maryland	Approved 07-09-09 @ 4:12 pm		
370	lil011@ucsd.edu	Linghan Li	Scripps Institution of Oceanography	Approved 07-10-09 @ 12:05 am		
371	wuhongyi1008@163.com	Hongyi Wu	University of Maryland	Approved 07-13-09 @ 10:10 pm		
372	akr@ucla.edu	Asa Rennermalm	UCLA	Approved 07-16-09 @ 1:28 am		
373	john.adler@colorado.edu	John Adler	CIRES	Approved 07-19-09 @ 7:56 am		
374	Christopher.A.Shuman@nasa.gov	Christopher Shuman	UMBC-GEST at NASA/GSFC	Approved 07-29-09 @ 11:45 am		
375	dva@geus.dk	Dirk van As	Geological Survey of Denmark and Greenland	Approved 07-29-09 @ 11:45 am		
376	jjaimoe@msn.com	JULIE MILLER	UNIVERSITY OF UTAH/ DEPARTMENT OF GEOGRAPHY	Approved 08-01-09 @ 4:54 pm		
377	ddwang@umd.edu	Dongdong Wang	Univeristy of Maryland	Approved 08-04-09 @ 7:08 pm		
378	decker.146@osu.edu	David Decker	Byrd Polar Research Center Ohio State University	Approved 08-24-09 @ 6:44 am		
379	wuhongyi1008@163.com	Hongyi Wu	University of Maryland	Approved 08-24-09 @ 6:46 am		
380	wuhongyi1008@hotmail.com	Hongyi Wu	University of Maryland	Approved 09-01-09 @ 11:41 pm		
381	konrad.steffen@colorado.edu	Koni		Approved 09-01-09 @ 11:40 pm		
382	chapman@atmos.uiuc.edu	William Chapman and John Walsh	University of Illinois at Urbana-Champaign	Approved 09-02-09 @ 11:43 am		
383	wuhongyi1008@163.com	HONGYI WU	University of Maryland	Approved 09-02-09 @ 1:37 pm		
384	boris.s.yurchak@nasa.gov	Boris Yurchak	NASA GSFC	Approved 09-04-09 @ 3:11 pm		

385	wuhongyi1008@163.com	HONGYI WU	University of Maryland	Approved 09-07-09 @ 5:24 pm	
386	wuhongyi1008@163.com	HONGYI WU	University of Maryland	Approved 09-07-09 @ 5:25 pm	
387	wuhongyi1008@163.com	Hongyi Wu	University of Maryland	Approved 09-08-09 @ 10:49 pm	
388	wuhongyi1008@163.com	Hongyi Wu	University of Maryland	Approved 09-08-09 @ 10:51 pm	
389	wuhongyi1008@163.com	Hongyi Wu	University of Maryland	Approved 09-08-09 @ 10:51 pm	
390	wuhongyi1008@163.com	Hongyi Wu	University of Maryland	Approved 09-08-09 @ 10:52 pm	
391	wuhongyi1008@163.com	hongyi wu	university of maryland	Approved 09-09-09 @ 9:51 am	
392	wuhongyi1008@163.com	hongyi wu	university of maryland	Approved 09-15-09 @ 12:09 am	
393	wuhongyi1008@163.com	hongyi wu	university of maryland	Approved 09-15-09 @ 12:09 am	
394	wuhongyi1008@163.com	hongyi wu	university of maryland	Approved 09-15-09 @ 12:09 am	
395	daniel.west@umontana.edu	Dan West	University of Montana, Deptartment of Geosciences	Approved 09-16-09 @ 8:47 am	
396	john.adler@colorado.edu	John Adler	CIRES	Approved 09-16-09 @ 5:24 am	
397	konrad.steffen@colorado.edu	koni	CIRES	Approved 09-16-09 @ 7:45 am	
399	alexk@iup.physik.uni-bremen.de	Alexander Kokhanovsky	University of Bremen	Approved 09-22-09 @ 9:34 am	
400	ngilson1@jhu.edu	Nicholas J Gilson	Johns Hopkins University	Approved 09-22-09 @ 9:36 am	
401	evanburgess@gmail.com	Evan Burgess	University of Utah	Approved 09-28-09 @ 11:07 pm	
402	daniel.west@umontana.edu	Dan West	University of Montana, Department of Geosciences	Approved 09-28-09 @ 11:08 pm	
403	daniel.mcgrath@colorado.edu	Daniel McGrath	CIRES	Approved 10-02-09 @ 12:47 am	
404	jonathan.day@bris.ac.uk	Jonathan Day	University of Bristol	Approved 10-06-09 @ 2:41 pm	
406	jack.saba@nasa.gov	Jack Saba	NASA/GSFC	Approved 10-08-09 @ 4:35 pm	
407	truffer@gi.alaska.edu	Martin Truffer	University of Alaska	Approved 10-08-09 @ 4:37 pm	

408	wuhongyi1008@163.com	Hongyi Wu	University of Maryland	Approved 10-10-09 @ 11:07 pm	
409	wuhongyi1008@163.com	Hongyi Wu	University of Maryland	Approved 10-10-09 @ 11:09 pm	
410	malin.johansson@natgeo.su.se	Malin Johansson	Stockholm University	Approved 10-13-09 @ 12:01 pm	
411	781714826@qq.com	Xiufang Zhu	university of maryland	Approved 10-13-09 @ 12:02 pm	
412	cfriberg@sfu.ca	Courtney Friberg	Sim Fraser University	Approved 10-14-09 @ 8:15 pm	
413	comissa@mail.ru	Irina	MSU	Approved 10-16-09 @ 12:07 pm	
414	pettitjoey@yahoo.com	Joey Pettit	Indiana State University	Approved 10-27-09 @ 9:27 pm	
415	wisecg@ku.edu	Clint Wiseman	University of Kansas, Physics Dept.	Approved 10-27-09 @ 9:28 pm	
416	seok@colorado.edu	Brian Seok	University of Colorado	Approved 10-30-09 @ 9:17 am	
417	circles@telenet.be	Dansercoer Dixie	Circles	Approved 11-01-09 @ 3:51 pm	
418	malin.johansson@natgeo.su.se	Malin	Stockholm University	Approved 11-07-09 @ 7:39 pm	
422	jplieberman@gmail.com	Jordan Pesses Lieberman	University of Georgia	Approved 11-18-09 @ 11:39 pm	
423	djl22@psu.edu	Derrick J Lampkin	Pennsylvania State University, Dept. of Geography	Approved 11-18-09 @ 11:41 pm	
424	pelkey@juniata.edu	Neil Pelkey	Junaita College	Approved 11-26-09 @ 6:49 pm	
425	xhu@londonmining.gl	Xiaogang Hu	London Mining Plc	Approved 12-02-09 @ 12:20 pm	
426	dps@colorado.edu	David Schneider	CIRES	Approved 12-02-09 @ 2:04 pm	
427	jjaimoe@gmail.com	JULIE MILLER	UNIVERSITY OF UTAH	Approved 12-03-09 @ 4:10 pm	
428	eeaal@leeds.ac.uk	amber Leeson	University of Leeds	Approved 12-04-09 @ 8:03 am	
430	jjaimoe@msn.com	jmiller	university of utah	Approved 12-12-09 @ 5:12 pm	
431	sjsk@nsidc.org	Siri Jodha KHALSA	NSIDC	Approved 01-06-10 @ 2:41 pm	
432	malin.johansson@natgeo.su.se	Malin Johansson	Stockholm University	Approved 01-08-10 @ 10:45 am	

433	david.podrasky@gi.alaska.edu	David Podrasky	Univ. of Alaska Geophysical Institute	Approved 01-16-10 @ 12:13 am	
434	lwang2@gmu.edu	Lingli Wang	Geroge Mason University	Approved 01-16-10 @ 12:14 am	
435	ernsdorf@uni-trier.de	Thomas Ernsdorf	University of Trier, Fac. of Geography/Geosciences, Dept. of Environmental Meteorology	Approved 02-05-10 @ 7:36 pm	
436	chad.steed@nrlssc.navy.mil	Chad Steed	Naval Research Laboratory	Approved 02-06-10 @ 7:14 pm	
437	yjz630@163.com	yjz	Jinan university, China	Approved 02-06-10 @ 8:27 pm	
438	yjz630@sina.com	Jianzhang Yu	Jinan University	Approved 02-10-10 @ 9:24 pm	
439	thomas.nagler@enveo.at	Thomas Nagler	Univ Innsbruck / ENVEO	Approved 02-13-10 @ 4:35 pm	
440	lisa.ho@colorado.edu	lisa ho		Approved 02-13-10 @ 4:34 pm	
441	crb50@cam.ac.uk	Catherine Baggs	Scott Polar Research Institute	Approved 02-18-10 @ 1:00 am	
442	liamdmathdude@hotmail.com	Russell		Approved 02-18-10 @ 11:47 pm	
443	liamdmathdude@hotmail.com	Russell		Approved 02-20-10 @ 1:57 am	
444	limaruss@sympatico.ca	Maria		Approved 02-20-10 @ 1:59 am	
445	liamdmathdude@hotmail.com	Russell		Approved 02-22-10 @ 11:26 pm	
446	cpchen@asiaa.sinica.edu.tw	Ben chen	Academia Sinica Institute of Astronomy and Astrophysics	Approved 02-24-10 @ 11:11 am	
447	adasgupt@uncc.edu	Aritra Dasgupta	University of North Carolina at Charlotte	Approved 02-24-10 @ 11:12 am	
448	xiaolei@atmos.umd.edu	XIAOLEI NIU	University of Maryland,College Park, Maryalnd,USA	Approved 02-24-10 @ 11:13 am	
449	xiaolei@atmos.umd.edu	XIAOLEI NIU	University of Maryland	Approved 02-25-10 @ 12:03 am	
450	m.a.brandon@open.ac.uk	Mark Brandon	The Open University	Approved 02-25-10 @ 11:03 am	
451	xiaolei@atmos.umd.edu	XIAOLEI NIU	University of Maryland,College Park, Maryalnd,USA	Approved 03-01-10 @ 5:02 pm	
452	adasgupt@uncc.edu	Aritra Dasgupta	University of North Carolina at Charlotte	Approved 03-01-10 @ 5:03 pm	
453	bfm@dartmouth.edu	Blaine Morriss	Dartmouth College	Approved 03-10-10 @ 7:47 am	

454	beal@dartmouth.edu	Sam Beal	Dartmouth College	Approved 03-04-10 @ 11:05 pm	
455	A.J.S.Farrar@sms.ed.ac.uk	Andrew Farrar	University of Edinburgh	Approved 03-06-10 @ 10:50 am	
457	pierre08250@msn.com	Huat	University	Approved 03-10-10 @ 7:46 am	
458	mlupker@crpg-cnrs.nancy.fr	Maarten Lupker	CRPG-CNRS FRANCE	Approved 03-21-10 @ 4:08 am	6.0M
459	lwang2@gmu.edu	Lingli Wang	George Mason University	Approved 03-23-10 @ 3:01 pm	72M
460	matthew.hoffman@nasa.gov	Matthew J. Hoffman	NASA Goddard Space Flight Center	Approved 03-27-10 @ 2:22 am	18M
461	jplieberman@gmail.com	Jordan Lieber-man	University of Georgia Climate Research Lab	Approved 03-29-10 @ 11:31 am	5.4M
462	khalid.hussein@colorado.edu	Khalid Hussein	ESOC, CIRES	Approved 03-31-10 @ 5:20 pm	3.4M
463	liamdmathdude@hotmail.com	Russell		Approved 04-12-10 @ 12:01 pm	40M
464	ddwang@umd.edu	Dongdong Wang	University of Maryland	Approved 04-12-10 @ 12:05 pm	57M
465	khalid.hussein@colorado.edu	Khalid Hussein	ESOC, CIRES	Approved 04-12-10 @ 12:08 pm	2.0K
466	mira.schmidt@hotmail.de	Schmidt	Technical University Braun-schweig	Approved 04-13-10 @ 10:23 am	2.0K
467	lwang2@gmu.edu	Lingli Wang	GMU	Approved 04-13-10 @ 10:21 am	71M
468	brandt@atmos.washington.edu	Richard Brandt	University of Washington Dept. of Atmospheric Sciences	Approved 04-14-10 @ 10:01 am	30M
469	khalid.hussein@colorado.edu	Khalid Hussein	ESOC, CIRES	Approved 04-14-10 @ 10:04 am	2.2M
470	princesss1085@yahoo.com	Lauren Ingram	Wenatchee Valley College at Omak	Approved 04-21-10 @ 10:06 pm	150M
471	mernild@lanl.gov	Sebastian H. Mernild	LANL	Approved 04-21-10 @ 11:13 pm	11M
472	mernild@lanl.gov	Sebastian H. Mernild	LANL	Approved 04-23-10 @ 11:50 am	4.4M
473	Thomas.Phillips@colorado.edu	Thomas Phillips	University of Colorado	Approved 04-23-10 @ 11:50 am	4.4M

Table 2.1: User requests for GC-Net data since January 2009. Approximately 5 Giga-Bytes of data were distributed via the FTP server for a total of 184 user requests.

2.3 GC-Net Citation List

This list represents publications that made use of Greenland Climate Network (GC-Net) data.

Abdalati, W. and K. Steffen, Greenland ice sheet melt extent: 1979-1999, J. Geophys. Res., 106(D24), 33,983-33,989, 2001.

Allison, I., et al., The Copenhagen Diagnosis,: Updating the World on the Latest Climate Change, The University of South Wales Climate Change Research Center (CCRC), Sydney, Australia, pp.60, ISBN 978-0-9873216-0-6, 2009.

Becker, O.O. and K. Steffen, Above Zero, Hatje Cantz Verlag, Austria, pp.175, ISBN 978-3-7757-2437-1, 2009.

Box, J.E., D.H. Bromwich1, B.A. Veenhuis, Le-S. Bai, J.C. Stroeve, J.C. Rogers, K. Steffen, T. Haran, S.-H.. Wang, Greenland ice sheet surface mass balance variability (1988-2004) from calibrated Polar MM5 output, J.Clim., 2005.

Box, J. E., Surface Water Vapor Exchange on the Greenland Ice Sheet Derived from Automated Weather Station Data, PhD Thesis, Department of Geography, University of Colorado, Boulder, CO, Cooperative Institute for Research in Environmental Sciences, 190 pp, 2001.

Box, J.E. and K. Steffen, Sublimation on the Greenland ice sheet from automated weather station observations, J. Geophys. Res., 106(D24), 33,965-33,982, 2001.

Bromwhich, D., J. Cassano, T. Klein, G. Heinemann, K. Hines, K. Steffen and J. Box, Mesoscale modeling of katabatic winds over Greenland with Polar MM5, Mon. Weather Review, 129, 2290-2309, 2001.

Cassano, J.J., J.E. Box, D.H. Bromwich, L. Li, and K. Steffen, Evaluation of Polar MM5 simulations of Greenland's atmospheric circulation, J. Geophys. Res., 106(D24), 33,867-33,890, 2001.

Cullen, N., and K. Steffen, Unstable near-surface boundary conditions in summer on top of the Greenland ice sheet., Geophys. Res. Lett., 28(23), 4491-4494, 2001.

Cullen, N.J., K. Steffen, and P. D Blanken, Nonstationarity of Turbulent Heat Fluxes at Summit, Greenland, Boundary-Layer Meteorology, DOI 10.1007/s10546-006-9112-2, 2006.

Davis, C.H. and D.M. Segura, An algorithm for time-series analysis of ice sheet surface elevations from satellite altimetry, IEEE Transactions on Geoscience & Remote Sensing, 39(1), 202-206, 2001.

Dassau, T.M., A. Sumer, S. Koeniger, P. Shepson, J. Yang, R. Honrath, N. Culen, K. Steffen, Investigation of the role of the snowpack on atmospheric formaldehyde chemistry at Summit, Greenland, J. Geophys. Res., 107(D19), ACH 9.1-14, 36, 2595-2608, 2002.

Fausto, R.S., A.P. Ahlstram, D. Van As, S.J. Johnsen, P.L. Langen , and K.Steffen, Improving surface boundary conditions with focus on coupling snow densification and meltwater retention in large-scale ice sheet models of Greenland, *J. Glaciol*., 55(193), 869-878, 2009.

Hall, D.K., J.E. Box, K.A. Casey, S.J. Hook, C.A. Shuman and K. Steffen, Comparison of satellite-derived and in-situ observations of ice and snow surface temperatures over Greenland, *Remote Sensing of the Environment*, 112(10), 3739-3749, 2008.

Hanna , E., P. Huybrechts, K. Steffen, J. Cappelen, R. Huff, Ch. Shuman, T. Irvine-Fynn, S. Wise, and M. Griffiths. Increased runoff from melt from the Greenland Ice Sheet: a response to global warming. *J. Climate*, 21, 331-341, DOI: 10.1175/2007JCLI1964.1, 2008.

Hanna,H., P.Huybrechts, I. Janssens, J..Cappelen, K. Steffen, and A. Stephens, Runoff and mass balance of the Greenland ice sheet: 1958–2003, J. Geophys. Res., 110, D13108, doi:10.1029/2004JD005641, 2005.

Hanna, E. and P. Valdes, Validation of ECMWF (re)analysis surface climate data, 1979-1998, for Greenland and implications for mass balance modeling of the Ice Sheet, Intern. J. Clim., 21, 171-195, 2001.

Helmig, D, J. Boulter, D. David, J. Birk, N. Cullen, K. Steffen, B. Johsnon, S. Oltmans, Ozone and meteorological boundary-layer conditions at Summit, Greenland, Atm. Environm., 36, 2595-2608, 2002.

Herzfeld, U.C., J.E. Box, K. Steffen, H. Mayer, N. Caine, and M. Losleben, A case study on the influence of snow and ice surface roughness on melt energy, Zeitschrift für Gletscherkunde und Glazialgeology, 39, 1-42, 2006.

Honrath, R.E. Y.Y. Lu, M.C. Peterson, J.E. Dibb, M.A. Arseault, N.J. Cullen, and K. Steffen. Vertical fluxes of NOx, HONO, and HNO3 above the snowpack at Summit, Greenland. Atm. Environm, 36, 2629-2640, 2002.

Klein, T., G. Heinemann, D. H. Bromwich, J. J. Cassano and K. M. Hines, Mesoscale modeling of katabatic winds over Greenland and comparisons with AWS and aircraft data, J. Met. Atmos. Phys., 8(1/2), 115-132, 2001.

Klein, T., G. Heinemann, Simulations of the katabatic wind over the Greenland ice sheet with a 3D model for one winter month and two spring months, Report of the DAAD/NSF project 315-PP, 1999.

Merlind, S.H., G. Liston, K. Steffen, and P. Chylek, Meltwater flux and runoff modeling in the ablation area of Jakobshavn Isbrae, West Greenland. *J. Glaciol.*, 56(195), 20-32, 2010.

Mernild, S.H., G.E. Liston, C.A. Hiemstra, K. Steffen, E. Hanna, and J.H. Christensen, Greenland Ice Sheet surface mass-balance modeling and freshwater flux for 2007, and in a 1995–2007 perspective, Hydrological Processes, DOI: 10.1002/hyp.7354, 2009.

Mernild, S.D., G.E. Liston, C.A., Hiemstra, C.A., and K. Steffen, Record 2007 Greenland ice sheet surface melt extent and runoff, *EOS*, 90, 13-14, (Jan 13), 2009.

Mernild, S., G. Liston, Ch. Hiemstra, K. Steffen, E. Hanna, and J.H. Christensen, Greenland Ice Sheet surface mass-balance modeling and freshwater flux for 2007, and in a 1995–2007 perspective. *J. Hydrometeorology*, 9, DOI: 10.1175/2008JHM957.1, 2008.

Mernild, S., G. Liston, Ch. Hiemstra, K. Steffen, Surface melt area and water balance modeling on the Greenland ice sheet 1995-2005, *J. Hydrometeorology*, 9, DOI: 10.1175/2008JHM957.1, 2008.

Mosley-Thompson, E., J.R. McConnell, R.C. Bales, Z. Li, P.-N. Lin, K. Steffen, L.G. Thompson, R. Edwards, D. Bathke, Local to regional-scale variability of annual net accumulation on the Greenland ice sheet from PARCA cores, J. Geophys. Res., 106 (D24), 33,839-33852, 2001.

Munneke, P.K., M. R. van den Broeke, C. H. Reijmer, M. M. Helsen, W. Boot, M. Schneebeli, and K. Steffen, The role of radiation penetration in the energy budget of the snowpack at Summit, Greenland. *The Cryosphere Discuss*., 3, 277-306, 2009.

Murphy, B. F., I. Marsiat and P. Valdes, Simulated atmospheric contributions to the surface mass balance of Greenland. J. Geophys. Res., 106, submitted, 2001.

Nghiem, S.V., , K. Steffen, G. Neumann, and R. Huff, Snow Accumulation and Snowmelt Monitoring in Greenland and Antarctica, International Association of Geodesy Publication, Dynamic Planet, Chapter 5, 31-38, 2007.

Nghiem,S,V., K. Steffen, G. Neumann, and R. Huff, Mapping of ice layer extent and snow accumulation in the percolation zone of the Greenland ice sheet, J. Geophys., Res., 110, F02017, doi:10.1029/2004JF000234, 2005.

Nghiem, S.V., K. Steffen, R. Kwok, and W.Y. Tsai, Diurnal variations of melt regions on the Greenland ice sheet, J. Glaciol., 47(159), 539-547, 2001.

Njastad, K., R. Armstrong, R.W. Corell, D.D. Jensen, K.R. Leslie, A. Rivera, Y. Tandong, J.D. Winther, and K. Steffen. Melting snow and ice: call for action, Center for Ice, Climate and Ecosystems, Norwegian Polar Institute, pp.92, ISBN 978-82-7666-264-1, 2009.

Nolin, A. and J. Stroeve, The Changing Albedo of the Greenland Ice Sheet: Implications for Climate Change, Annals of Glaciology, 25, 51-57, 1997.

Orr, A., E. Hanna, J. Hunt, J. Cappelen, K. Steffen and A. Stephens, Characteristics of stable flow over southern Greenland, *Pure and Applied Geophysics* (PAGEOPH), 161(7), 2004.

Painter, T.H., N.P. Molotch, M. Cassidy, M. Flanner, and K. Steffen, Contact spectroscopy for determination of stratigraphy of snow grain size, *J. Glaciol*, 53(180) 121-127, 2007.

Parry, V., P. Mair, J. Scott, B. Hubbard, K. Steffen, and D. Wingham, Investigations of meltwater refreezing and density variations in the snowpack and firn within the percolation zone of the Greenland Ice Sheet, Ann. Glaciol., 46, 621-68, 2007.

Rial., J., C. Tang, and K. Steffen, Glacial Rumblings from Greenland's Jakobshavn Ice Stream, *J. Glaciolo*., in press, 2009.

Serreze, M., J. Key, J. Box, J. Maslanik, and K. Steffen, A new monthly climatology of global radiation for the Arctic and comparison with NCEP-NCAR reanalysis and ISCCP-C2 field, J. Climate, 11, 121-136, 1998.

Shuman, C., K. Steffen, J. Box, and C. Stearn, A dozen years of temperature observations at the Summit: Central Greenland automatic weather stations 1987-1999, J. Appl. Meteorol., 40(4),741-752, 2001.

Smith, L.C., Y. Sheng, R.R. Foster, K. Steffen, K.E. Frey, and D.E. Alsdorf, Melting of small Arctic ice caps observed from ERS scatterometer time series, Geophys. Res. Lett., 30(20), CRY 2-14, 2003.

Steffen, K., S.V. Nghiem, R. Huff, and G. Neumann, The melt anomaly of 2002 on the Greenland Ice Sheet from active and passive microwave satellite observations, Geophys. Res. Lett., 31(20), L2040210.1029/2004GL020444, 2004.

Steffen, K., and J.E. Box, Surface climatology of the Greenland ice sheet: Greenland climate network 1995-1999, J. Geophys. Res., 106(D24), 33,951-33,964, 2001.

Steffen, K., W. Abdalati, and I. Serjal, Hoar development on the Greenland ice sheet, J. of Glaciology, 45(148), 63-68, 1999.

Steffen, K., J. E. Box and W. Abdalati, Greenland climate network: GC-Net, CRREL, 98-103 pp., 1996.

Stroeve, J., Assessment of Greenland Albedo Variability from the AVHRR Polar Pathfinder Data Set, J. Geophys. Res., 106(D24), 33,989-34,006, 2001.

Stroeve, J., and A. Nolin, 1997. The changing albedo of the Greenland ice sheet: implications for climate modeling, Ann. of Glaciol., 25, 51-57.

Stroeve, J, J. E. Box, J. Maslanik, J. Key, C. Fowler, Intercomparison between in situ and AVHRR Polar Pathfinder-derived surface albedo over Greenland, Remote Sensing of the Environment, 75(3), 360-374, 2001.

Thomas, R., and PARCA instigators, Program for Arctic Regional Climate Assessment (PARCA): Goals, key findings, and future directions, J. Geophys. Res., 106(D24), 33,691-33706, 2001.

Thomas, R.H., W. Abdalati, E. Frederick, W.B. Krabill, S. Manizade, and K. Steffen, Investigation of surface melting and dynamic thinning on Jakobshavn Isbrea, Greenland, J. Glaciol., 49(165), 231-239, 2003.

Wang, L., M. Sharp, B. Rivard, and K. Steffen, Melt duration and ice layer formation on the Greenland ice sheet, 2000-2004, J. Geophys. Res., 112, F04013, doi:10.1029/2007JF000760 2007.

Zwally, H.J. W. Abdalati, T. Herring, K. Larsen, J. Saba, and K. Steffen. Surface melt-induced acceleration of Greenland ice-sheet flow, Science, 297, 218-222, 2002.

3. Results

3.1 Swiss Camp Climatology: 1991-2009

3.1.1 Temperature

The mean annual air temperature at Swiss Camp is -12.3° C (1991-2009), with the coldest monthly temperature in February (-32° C) and the warmest monthly temperature in July (Fig. 3.1.1). Summer months with above freezing occurred in 1995, and from 1997– present.

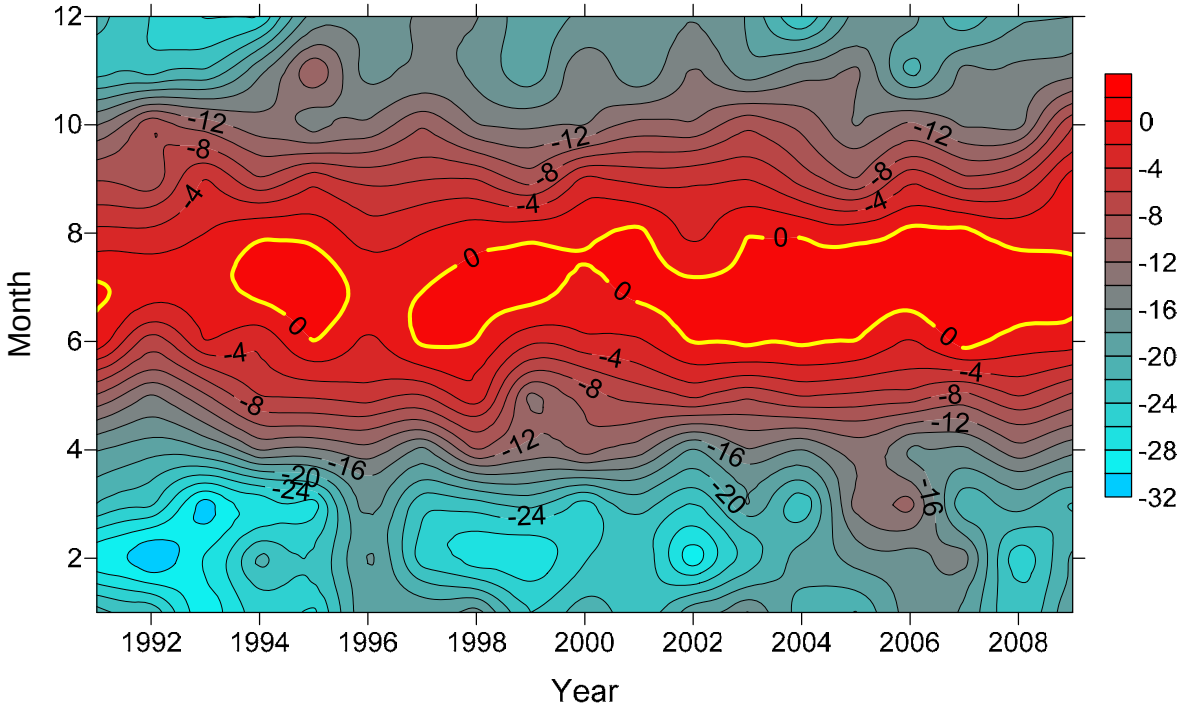

Figure 3.1.1: Interannual variability of monthly mean air temperatures (1991 – 2009) at the Swiss Camp, located at the equilibrium line altitude on the western slope of the Greenland ice sheet.

The mean annual temperature has increased by 3.8 ºC using a linear regression model as shown in Figure 3.1.2. The minimum temperature in 1992 was the result of the aerosol loading caused by the Mt. Pinatubo eruption. The linear regressing model at 95% confidence shows that the Pinatubo cooling and also the subsequent warming from the mid 90's were outside the 95% level of confidence. The warming that occurred since 2000 to present shows approximately the same trend then the 18-year time series. The warmest mean annual temperature was recorded with -10.3º C in 2007. The lastest two years of the time series show a slight cooling as part of the climate variability

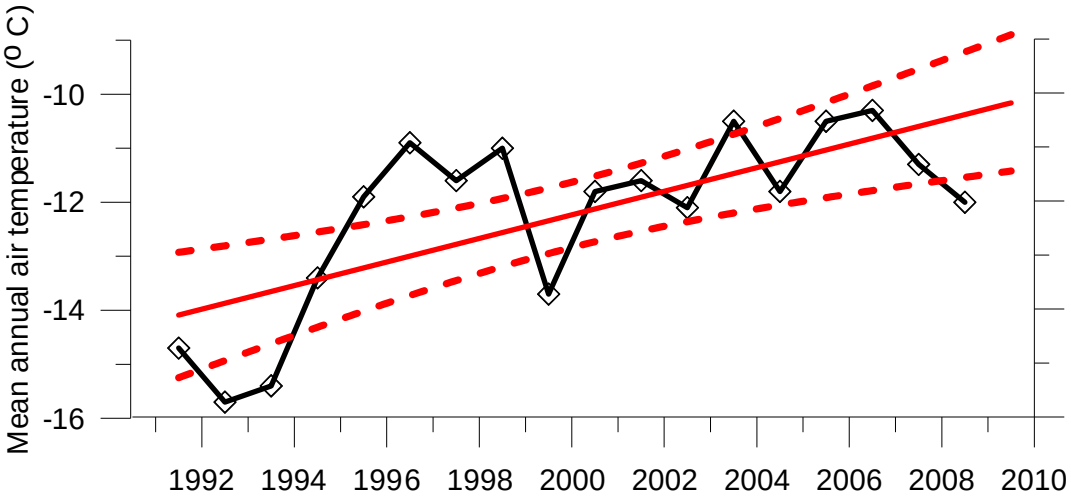

Figure 3.1.2: Swiss Camp mean annual temperature 1991 – 2009 (black line) with a linear regression model (red line) and 95% confidence levels (dashed red lines).

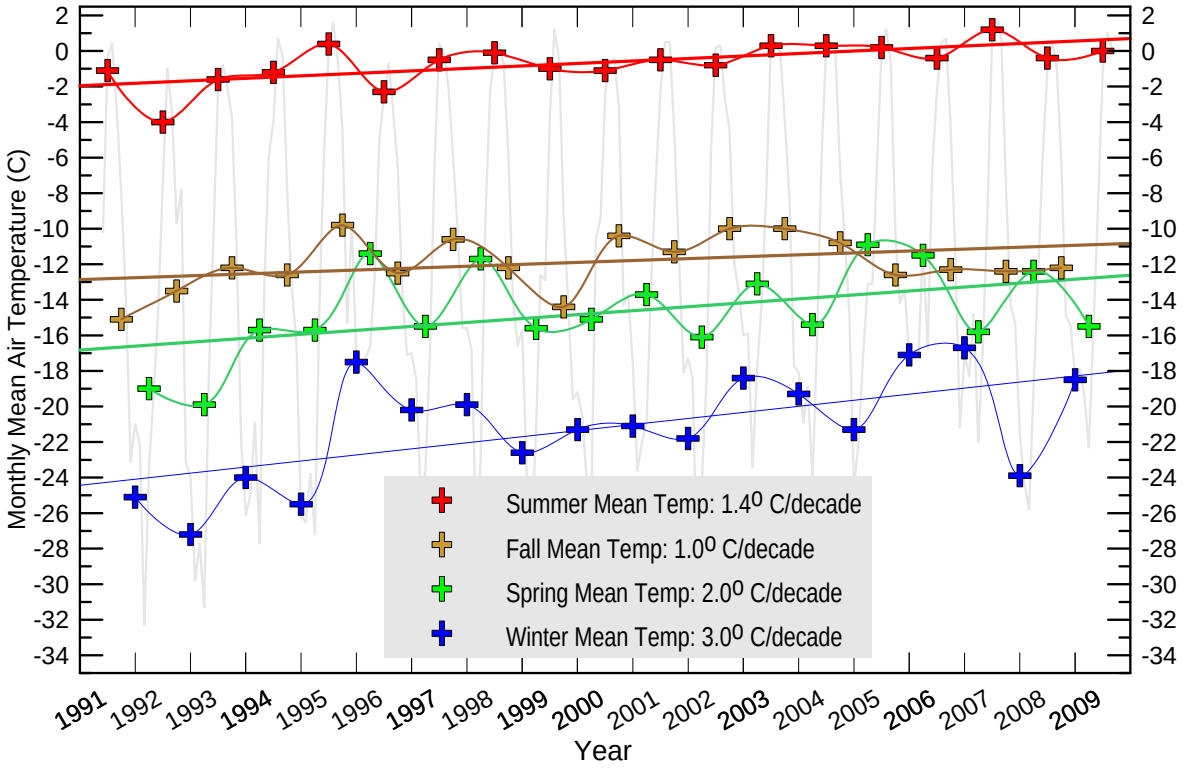

Figure 3.1.3: Swiss Camp mean monthly temperatures, and mean seasonal temperatures for summer, spring, fall, and winter for 1991 – 2009

The statistical analysis of the Swiss Camp air temperature record reveals large interannual variability in all seasons with increasing temperatures throughout the recording period (Fig. 3.1.3). The mean spring temperature increased from -17.5º C to -12.5º C, and fall temperature increased from -12.7º C to -11.0º C between 1991 and 2009, using a linear model. The winter temperature showed the largest increase of 6.3º C, whereas summer temperatures increased 2.3º C during the 16 years (1991 – 2008). The climate record at Swiss Camp shows a clear warming trend that started around 1995, consistent with the Arctic warming discussed in Fig. 1.1.

3.1.2 Radiation

Radiation has been monitored continuously at Swiss Camp since 1993. The time series of mean monthly net radiation values is shown in Figure 3.1.4 (1993 – 2009). The largest monthly mean net radiation is found in summer 2007 (> 60 W m^{-2}), coincident with air temperatures above freezing, indicating a strong albedo-feedback mechanism at the ELA. Most of the annual snow cover melted and the bare ice surface was exposed, reducing the monthly albedo value to 0.4 (Fig.3.1.5).

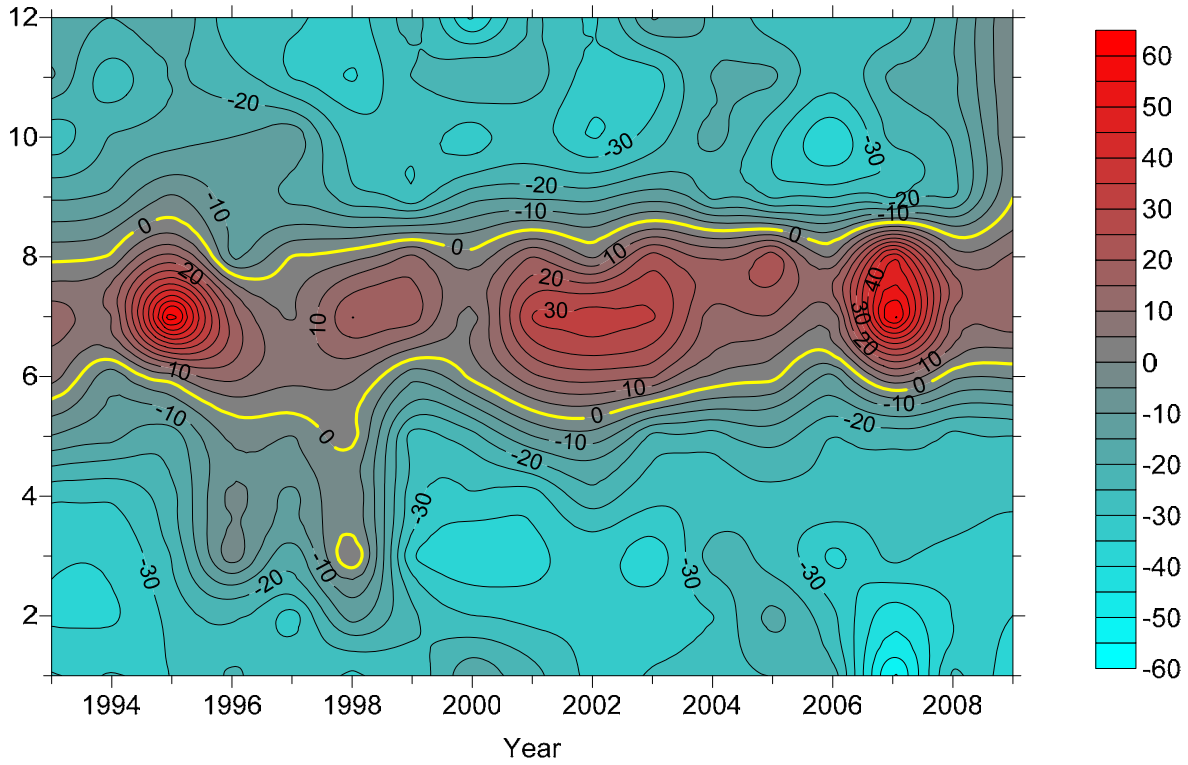

Figure 3.1.4: Interannual variability of monthly net radiation at the Swiss Camp (1993-2009).

It is worth discussing the three anomalous periods 1995, 1998, and 2001-2009 (Fig. 3.1.4). The summer season is characterized by a positive net radiation flux, which is indicative of the length of the melting season. High net radiation values can either be the result of low albedo values (i.e., 2003-2009, Fig. 3.1.5), reduced cloudiness (increase in insolation), or increase in atmospheric temperatures (increase in long-wave radiation). The mean summer net radiation has been higher during the new millennium (30 W m^{-2}) compared to the previous decade, with the exception of record high values in 1995, as a result of increased atmospheric temperatures leading to increase in surface melt (albedo reduction).

3.1.3 Accumulation and Ablation

Interannual variability of snow accumulation varies between 0.07 and 0.70 m water equivalent (w.e.), whereas the snow and ice ablation varies between 0 and 1.7 m (w.e.) for the time period 1990-2009. The mean net surface mass balance hovered around zero in the 90's with large deviations from the mean (Fig. 3.1.6), and a net mass loss is apparent starting in 2001 to present. The equilibrium line altitude (ELA) is no longer located at Swiss Camp (1100 m elevation) with a net surface loss of 4.0 m, and moved tent's of kilometers inland.

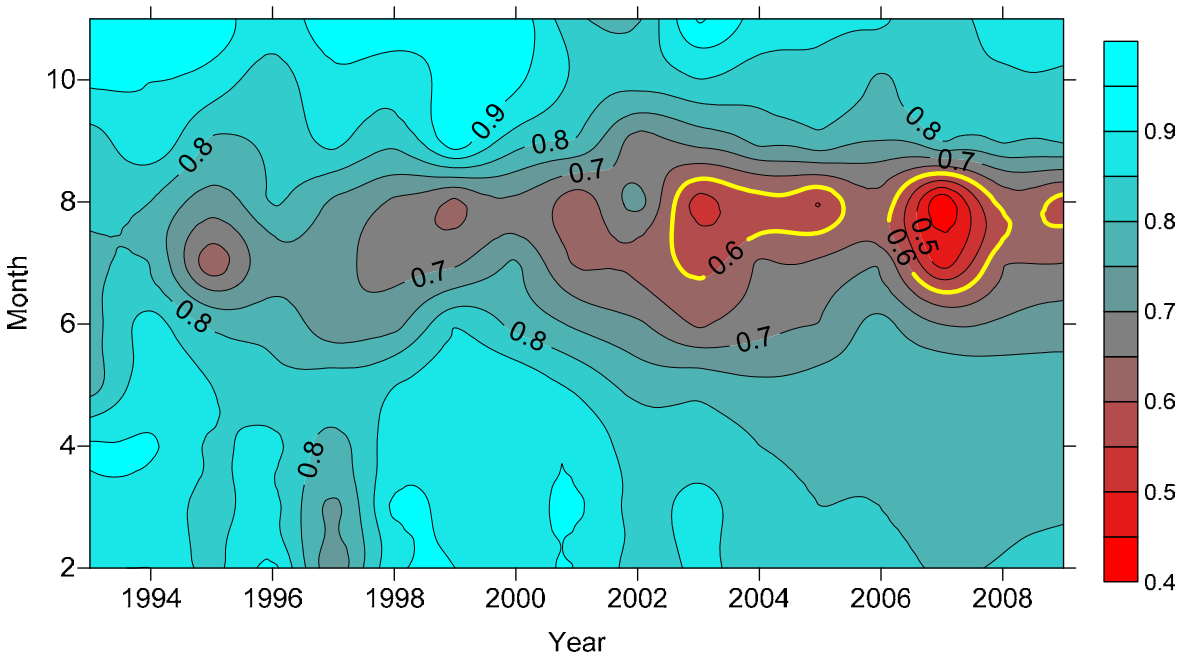

Figure 3.1.5: Interannual variability of monthly mean albedo at the Swiss Camp (1993 – 2009).

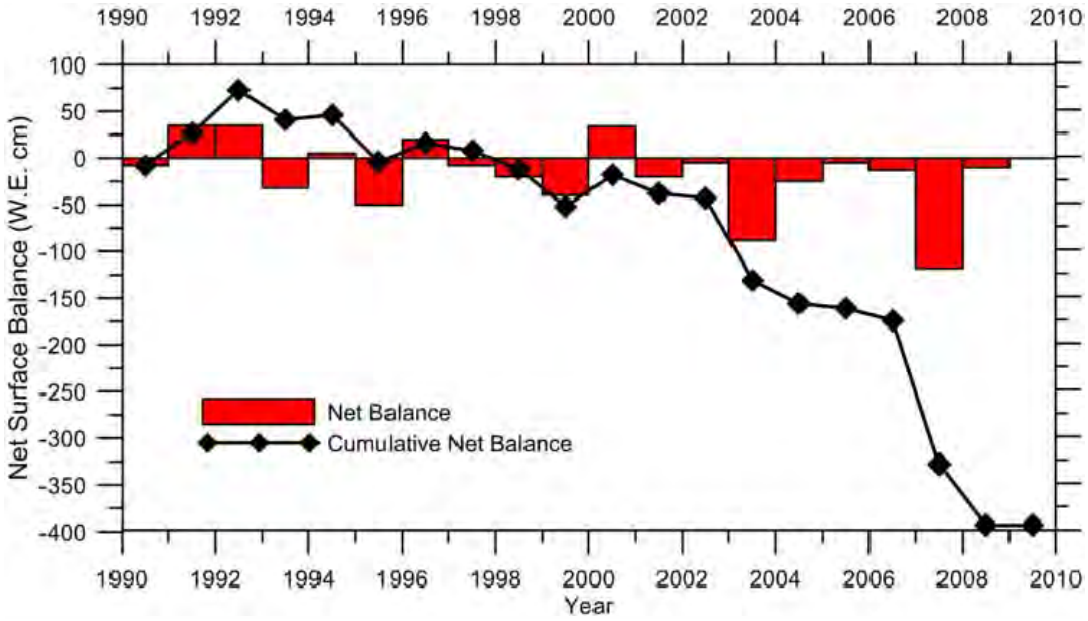

Figure 3.1.6: Net surface mass balance for the Swiss Camp location (red bars) total degree day totals normalized by the mean over the time period 1991-2009, and cumulative net balance (thick black line).

3.2 Moulin and Englacial Modelling

Three models were established to understand the influence of melt water on the englacial temperature of the ablation zone. The Sermeq Avannarleq outlet glacier immediately to the North of Jakobshavn where the University of Colorado currently has four Greenland Climate Network (GCNet) Automatic Weather Stations (AWS hereafter) JAR 1, JAR2, Swiss Camp and Crawford Point was used as a study site. Three individual models were developed in order to understand the processes involved:

1. The Fuzzy Logic Moulin Risk model was developed in order to understand the distribution of water infiltration into the ice as a function of Moulin locations and water availability in the ablation zone.
2. The dual-column cryo-hydrologic heat exchange model was designed to understand the interaction between the cryo-hydrologic system and the ice. The model was used to understand the influence of the annual melt season, the surface snow cover in winter and the temperate ice at the ice/water interface.
3. The cryo-hydrologic flowline model was used to estimate the influence of the surface melt on an entire ice sheet. This model allows us to estimate the temperature increase we can expect due the equilibrium line rising and increasing the area of the ablation zone.

3.2.1 Fuzzy Set Surface Melt Model

According to *Corne et al.* (1999) fuzzy set theory is a valid approach to understand an ill-defined phenomenon in glaciology. More established methods such as low-order nonlinear differential equations optimized by inversion perform better in well studied areas due to the fact that they have more parameters (*Clark & Murray*, 1995). In unknown areas the close fit to the known variables can become a handy cap: Fuzzy set theory results are less wrong in these locations as they do not search for the best fit model. According to fuzzy set theory there are problems where there is no best fit model. In the case studied here, where the reliability of the map, the accuracy of the moulins and the digital elevation model are unknown, fuzzy set theory is a valid approach to get a first estimate of the distribution of moulins and the driving forces that cause a moulin to develop in one place but not in another.

Despite the three variables aspect, elevation and slope being selected for their easy accessibility and using the two most simple operators ‘union’ and ‘intersection’ it could be shown, that moulin locations can be discriminated from a study site such as the Sermeq Avannarleq Glacier. A resulting map of the fuzzy set approach can be viewed in Figure 3.2.1. Using a flowline derived from the *Rignot et al.* (2006) velocity analysis the probability of water penetrating the ice along the flowline could be calculated. This was used as a surface boundary condition for the along flow model. The resulting probabilities for three different fuzzy maps are shown in Figure 3.2.2. Despite the three model approaches showing different heights of probability, their peaks are at the same locations along the flowline.

3.2.2 Dual Column Model

During the melt season large amounts of melt water are generated at the surface of the ablation zone. The water run-off and penetrates the ice by means of fractures, crevasses and moulins (*Fountain and Walder*, 1998). The water runs through conduits englacially until it reaches the bed of the ice sheet from where it flows to the margin and into the ocean. As the water runs through the ice over a period of 8-12 weeks depending on the length of the melt season, it is prevented from freezing due to turbulent flow. The ice at the ice/water interface warms therefore to the pressure melting point resulting in a temperature gradient between locations close to water supply and insulated areas. A warming of the ice is the result. At the end of the season the ice at the conduits consists of a fraction of water (<0.5%, *Duval*, 1977). As this water freezes it releases latent energy. The approach used in the dissertation involves a dual-column model, in which the first column is a modified column model (*Budd*, 1961; *Hooke*, 1977) for glacier ice to include a cryo-hydrologic heat exchange term. The second column represents the cryo-hydrologic system. For simplicity measures we view the ice and cryo-hydrologic systems as dual overlapping continua, as in the dual-porosity models for flow in fractured rock (e.g. *Barenblatt*, 1962). At larger scales, equations for spatially averaged temperatures may be written for each continuum, incorporating an aggregated exchange flux with the other continuum. The results of this model indicate three major findings:

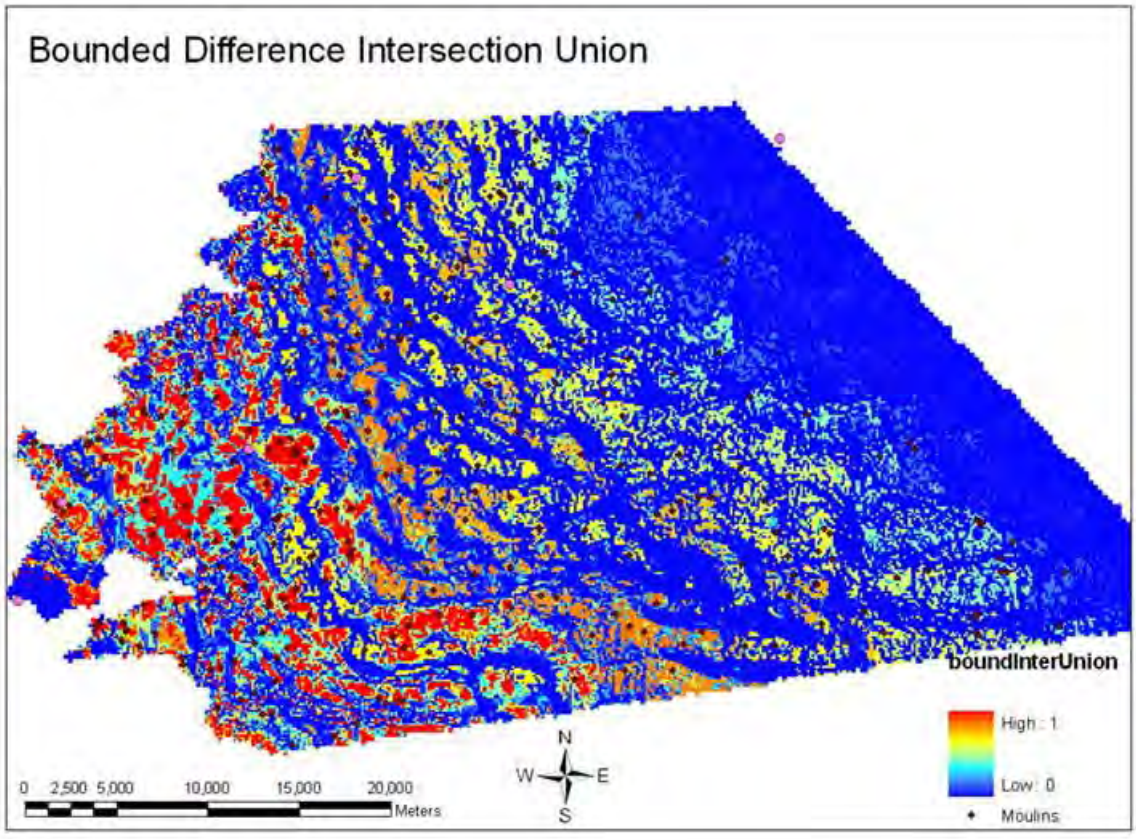

Figure 3.2.1: The bounded difference approach using union to combine slope and aspect. The result was intersected with the elevation membership function.

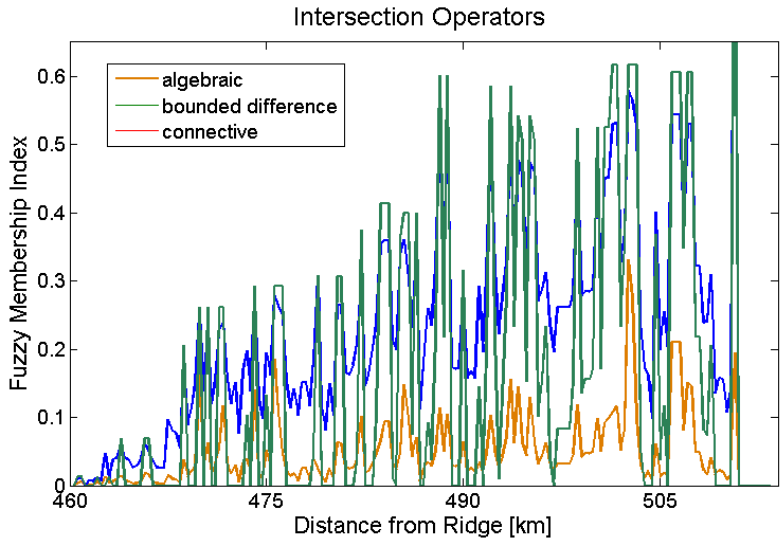

Figure 3.2.2: The three intersection approaches are compared for the moulin membership along the Sermeq Avannarleq flow line. The bounded difference approach results in the highest degrees of membership whereas the connective has the lowest.

1) The dual-column cryo-hydrologic model can warm ice within two decades, where the common model needs centuries to thousands of years. Due to the melt water the temperature of the ice in the ablation zone can adapt more rapidly to a changing climate (Figure 3.2.3).
2) Despite there being a seasonality in the generation of melt water, the ice temperatures at depths of 100m and more show no seasonality in temperature when the new steady state temperature is reached (Figure 3.2.3).
3) The ice sheet temperature is not influenced as much by the volume of melt but of the distribution of the cryo-hydrologic network. A denser network can warm the ice to a higher temperature in less time (Figure 3.2.4).

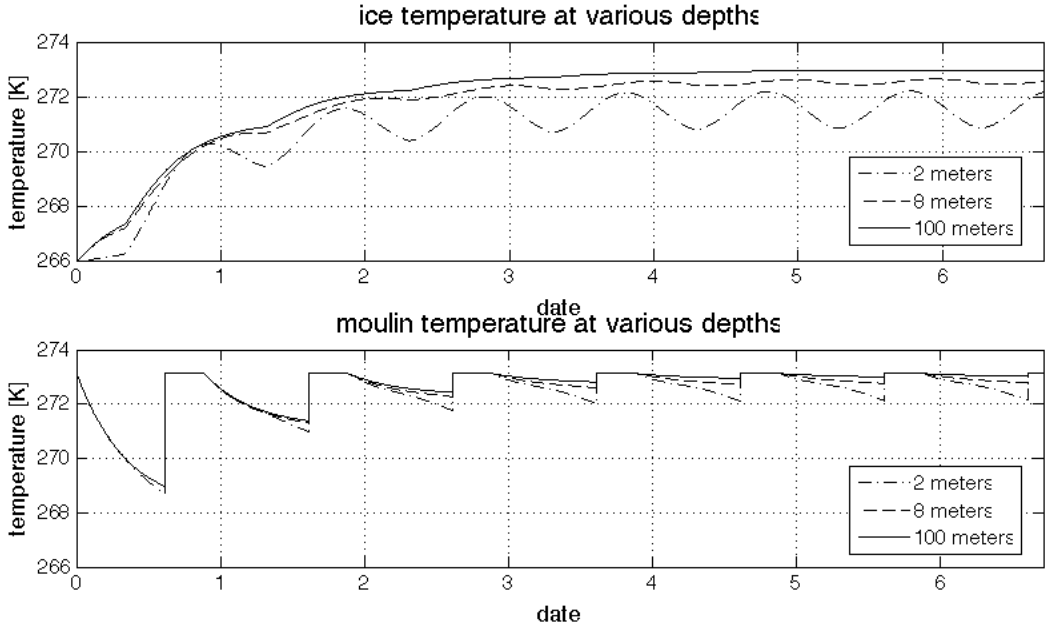

Figure 3.2.3: The top image describes the temperature at three depths in the ice column. The temperature at 2m depths keeps a seasonality, which is influenced by the surface air temperature. The seasonality at larger depths however is lost despite having a clear seasonality in the temperature in the cryo-hydrologic column (lower image). The cooling of the ice becomes less with time in the second column due to the warming of the ice.

3.2.3 FlowLine Model

In a final part of the dissertation the cryo-hydrologic heat exchange term is implemented into a simple flowline model in order to simulate the influence of cryo-hydrologic warming on the englacial temperature profile along the flowline of the Sermeq Avannarleq Glacier in western Greenland. The temperature profile is first computed at the divide. Subsequently, the calculated temperatures at upstream columns are used in the specification of the horizontal advection term in the immediately downstream columns. The temperature calculations are advanced sequentially along the downstream direction. A similar approach is taken as in the Budd column model including a diffusivity term, horizontal and vertical advection and internal deformation (*Funk et al.*, 1994). *The Fausto et al.* (2009a) lapse rate of 0.7K/100m was used. JAR2 was used as an anchor point. In addition the increased ablation and accumulation rates described by *Fausto et al.* (2009b) were used, increasing the velocity.

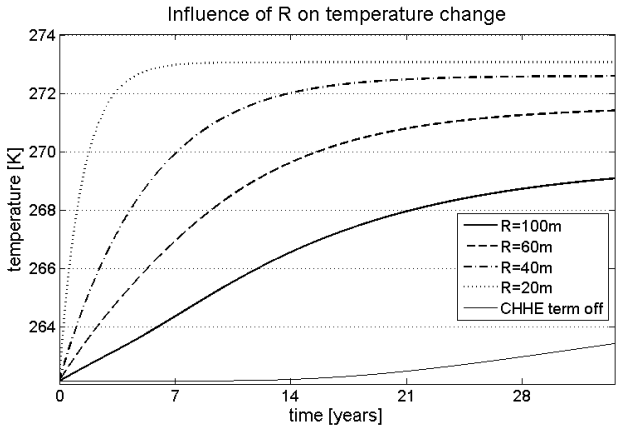

Fig Figure 3.2.4: R is the average distance between the conduits, fractures, crevasses and moulins. The black curves indicate that with increasing R it takes longer to reach a new steady state temperature. Large R-values result in lower new steady state temperatures. The "CHHE term off" curve indicates that the ice temperature at 100m does not react to a change in the climate within the same amount of time. The cryo-hydrologic term therefore allows the ice temperature to adapt to a changing climate more rapidly.

The flowline model result show that neglecting the influence of melt water in the ablation zone which leads to an underestimation of the ice temperature (Figure 3.2.5). The cryo-hydrologic heat exchange term has the largest influence in regions at the equilibrium line. Cold ice from the accumulation zone flows into this region, the percolating melt water can elide the cooling. In a changing climate where areas that were formally in the accumulation zone and hence containing cold ice become exposed to melt, the ice's temperature can be raised. Without the inclusion of melt water it takes centuries for the ice sheet to adjust to the changes due to the slow processes of advection and heat conduction. The inclusion of melt water as a form of energy transport into the ice speeds the process of the ice sheet up to decades rather than centuries.

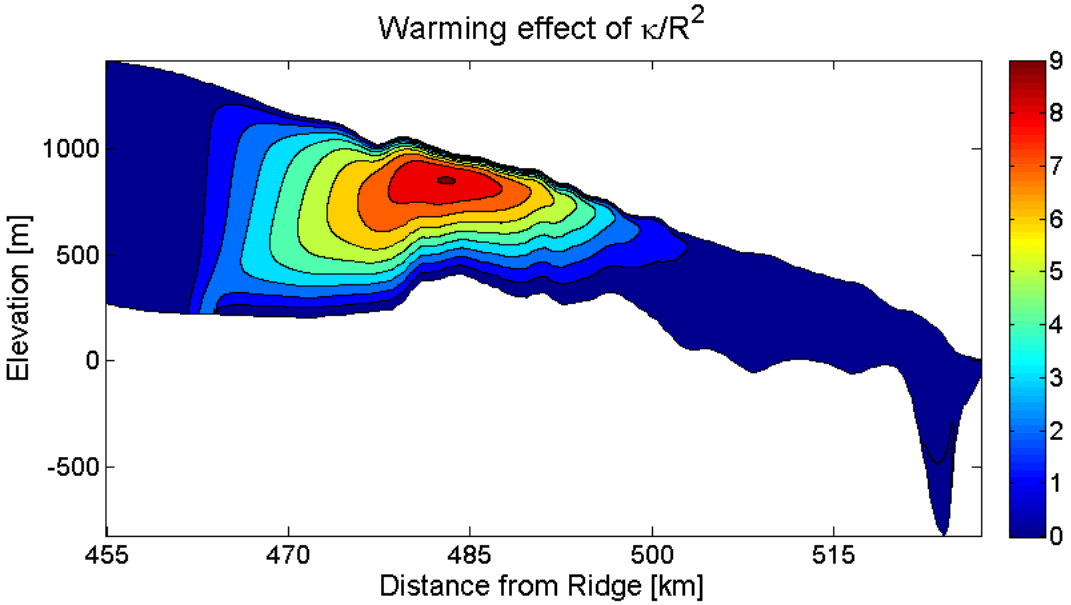

.

Figure 3.2.5: Using the best estimates for the current climate, the geothermal heat flux as well as ice velocity. The comparison of the model runs with the cryo-hydrologic term on as well as off shows that the inclusion of the melt water raises the ice temperature by as much as 9K! We therefore conclude that the underestimation of ice velocities in current models may well be caused by underestimating the ice temperature.

3.2.4 Future Work

Despite using the common topographic features elevation, slope and aspect Moulin risk maps could be produced which are credible. The physical explanations however are not satisfactory. It is therefore proposed here to use other more exact and physically appropriate variables. These include:

1) The second derivative of elevation and hence the slope of the slope. The second derivative is proportional to the shear stress. High values would therefore indicate a high risk for crevassing and hence an increased probability of Moulin development.
2) Basin size could be used to calculate where large amounts of melt water can collect. This would allow the inclusion of water availability.

The possibility of the interaction of cold air in the conduit system during autumn and winter has been neglected in the dual column approach. The possibility of cold air infiltrating the ice sheet has to be considered in the future. In addition the idea of water entering the ice by means of moulins has to be reconsidered. *McGrath and Colgan (*2010) calculated that approximately 65% of the generated melt water of the catchments area enters the ice through the CU Moulin. 7% evaporates and the remaining 28% infiltrates the ice sheet through cracks. In addition the model presented here denotes the importance of a dense cryo-hydrologic network rather than the importance of large amounts of water. In future work the focus will be on the development and maintenance of the englacial river network using the Spring Hutter equations as well as *Clarke*'s (2003) and *Badino*'s (2002b) insights.

The flowline model has indicated the large influence of melt water and the possibility of rapid temperature changes due to the changing climate. In future work the focus will be on the influence of increased precipitation, the geo thermal heat flux and possible two dimensional approaches to understand the temperature profile in a catchment basin. In addition we propose to develop a fully transient enthalpy based model.

3.3 Glaciohydrology

3.3.1 Theoretical motivation

The velocity observed at a glacier's surface is the result of three mechanisms of ice flow: (i) internal deformation, (ii) basal sliding and (iii) basal sediment deformation. *In situ* observations in Western Greenland show that the basal sliding velocity of marginal ice varies with surface meltwater input to the englacial system on synoptic time-scales (*Zwally et al.*, 2002; *Bartholomew et al.*, in press). The relatively rapid response of basal sliding to perturbations in ice sheet glaciohydrology contrasts with the more lengthy responses (i.e. centurial to millennial) of internal and basal sediment deformation velocities to changes in glaciohydrology (*Marshall*, 2005). Recent interferometric synthetic aperture radar (InSAR) measurements have confirmed that a seasonal basal slide cycle is spatially widespread in the marginal ice of Western Greenland (*Joughin et al.*, 2008).

The suggestion that changes in glaciohydrology may have been responsible for the eventual demise of the Scandinavian Ice Sheet (*Arnold and Sharp*, 2002), combined with projections of increased Greenland Ice Sheet surface meltwater production over the next century (*Hanna et al.*, 2005), provide an impetus to conceptually understand and quantify the seasonal basal slide cycle of the Greenland Ice Sheet. Describing the relation between surface meltwater production and basal sliding, as well as quantifying the temporal and spatial distribution of basal sliding variability, are pressing objectives for three main reasons: (i) to establish whether a non-linear relation between meltwater input and basal sliding exists, (ii) to reduce uncertainties in satellite-derived InSAR mass-balance estimates due to intra-annual basal sliding variations, and (ii) to reduce uncertainties in the projected dynamic contribution of the Greenland Ice Sheet to sea level rise due to inter-annual basal sliding variations.

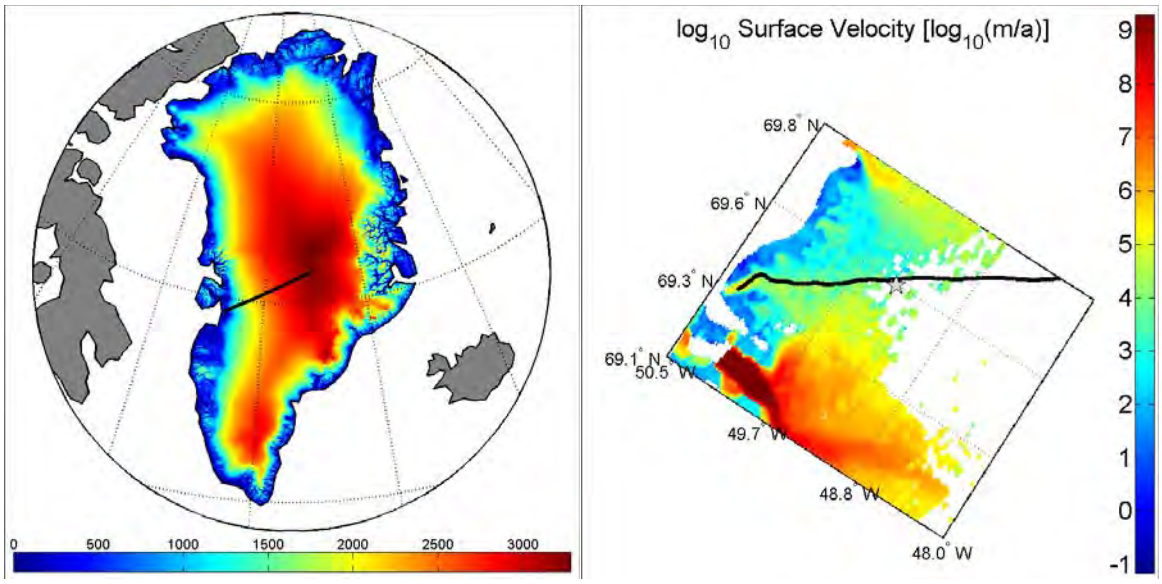

Figure 3.3.1 – Left: The Sermeq Avannarleq flowline overlaid on observed ice surface elevation (Scambos and Haran, 2002). Right: The terminal portion of the flowline, just north of Jakobshavn Isbrae, overlaid on inferred ice surface velocity (Rignot and Kanagaratnam, 2006). Swiss Camp is identified with a star.

3.3.2 Empirical motivation

CU-ETH ("Swiss") Camp is situated along the terminal portion of the Sermeq Avannarleq ("Dead") Glacier flowline in Western Greenland (Figure 3.3.1). This 530.5 km flowline runs from the main ice divide of the Greenland Ice Sheet (at 71.54 °N, 37.81 °W) to the glacier's tidewater terminus (at 69.37 °N, 50.28 °W). Twelve years (1996 to 2008) of differentially-corrected *in situ* global positioning system (GPS) data demonstrates that Swiss Camp experiences an annual velocity cycle (*J. Zwally*, personal communication). This annual cycle is comprised of four phases: (i) a spring speedup event, (ii) a summer slowdown event, (iii) a fall recovery event (in which velocities return to winter mean velocity from fall minimum velocity) and (iv) sustained winter speeds.

We can efficiently characterize the annual velocity cycle at Swiss Camp using a simple function comprised of two Gaussian curves superimposed on the mean winter velocity, where one curve represents the summer speedup and the other curve represents the fall slowdown (Figure 3.3.2). Gaussian curves were chosen to represent the summer and fall velocity anomalies because the amplitude, width and timing of these curves can be independently parameterized. Thus, for each of the twelve years for which data is available, the surface velocity (u_s) at Swiss Camp on a given Julian Day (j) may be characterized by three terms:

$$u_s = u_w + (u_{max} - u_w) \cdot \exp\left(\frac{j - J_{max}}{D_{max}}\right)^2 - (u_w - u_{min}) \cdot \exp\left(\frac{j - J_{min}}{D_{min}}\right)^2 \qquad \text{Eq. 3.3.1}$$

The winter velocity of a given year (u_w = 113.3 ± 1.7 m/a) was calculated as the mean of observed velocity values between JD 300 and 100. The summer maximum (u_{max} = 158.0 ± 43.2 m/a) and fall minimum (u_{min} = 99.2 ± 8.0 m/a) of a given year velocities were taken from 3-day mean GPS velocity observations. The remaining four parameters specify the timing and shape of the summer speedup and fall slowdown curves and were manually evaluated for each year. J_{max} (209.5 ± 8.8) and J_{min} (246.8 ± 9.4) represent the Julian Date of summer maximum and fall minimum velocity respectively. D_{max} (15.0 ± 7.7 d) and D_{min} (22.5 ± 2.6 d) represent the duration of the

summer and fall velocity anomaly. The mean value of each parameter can be used to model the mean annual ice velocity cycle at Swiss Camp over the twelve year period (Figure 3.3.2).

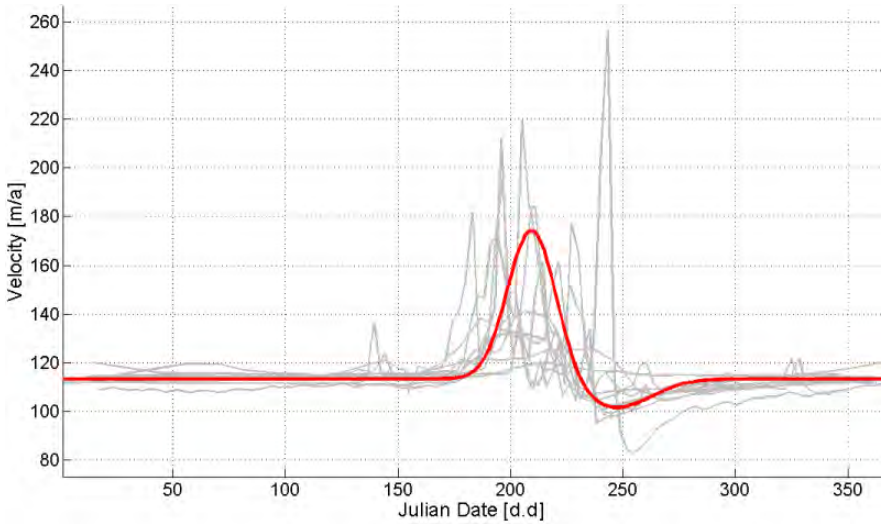

Figure 3.3.2 – Twelve years (1996 to 2008) of surface ice velocity versus Julian Date at Swiss Camp (grey lines) and the mean modeled annual velocity cycle (red line) according to Equation 3.3.1.

3.3.3 Alpine glaciohydrology theory

Alpine glacier studies suggest that changes in basal sliding velocity are due to changes in the rate of water storage (i.e. total glacier water inputs minus outputs; *Kamb et al.*, 1994; *Fountain and Walder*, 1998; *Anderson et al.*, 2004; *Bartholomaus et al.*, 2008), rather than changes in effective englacial water pressure (P_w) relative to ice pressure (P_i), or "floatation fraction" (i.e. P_w/P_i). This explains why meltwater pulses can initiate bursts of basal motion, while sustained meltwater input, which leads to the establishment of efficient subglacial conduits and low subglacial water pressures, does not lead to sustained basal slide (*Bartholomaus et al.*, 2008). Changes in the rate of water storage (dS/dt) are due to changes in both meltwater production (i.e. glacier "input") and subglacial water transmission ability (i.e. glacier "output"). Two distinct basal sliding states exist in an alpine glacier: (i) when meltwater input exceeds subglacial transmission ability, and (ii) when transmission ability exceeds meltwater input (*Anderson et al.*, 2004).

At the beginning of the melt season surface meltwater inputs exceed the transmission capacity of the nascent subglacial system. This results in the pressurization of subglacial conduits and basal sliding (*Fountain and Walder*, 1998; *Anderson et al.*, 2004; *Bartholomaus et al.*, 2008). The subglacial water system grows throughout the melt season. At the end of the melt season, basal sliding velocities begin to decrease once meltwater inputs fall below the water transmission capacity of the now established subglacial water system (i.e. dS/dt is negative; *Anderson et al.*, 2004). Empirical observations from alpine glaciers suggests that the rate of change in water storage (dS/dt) is proportional to basal sliding velocity (u_b) according to (where k and p are integers):

$$u_b \approx k \cdot \left(\frac{dS}{dt}\right)^m \qquad \text{Eq. 3.3.2}$$

3.3.4 Hydrology model

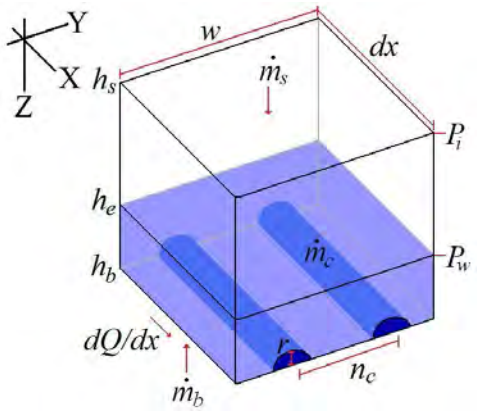

Figure 3.3.3 – Graphical overview of the 1D hydrology model framework (Equations 3.3.3 to 3.3.5).

We have generated a 1D (flowline) hydrology model, predicated on alpine glacio-hydrology theory, to investigate the annual velocity cycle at Swiss Camp in the context of changes in the rate of water storage (dS/dt). Once accounting for bulk ice porosity, changes in englacial water height (h_e) can be taken as a proxy for changes in total glacier storage (dS/dt; Equation 3.3.3). The rate of change in englacial water height ($dh_e/dt \approx dS/dt$) can be translated into basal sliding velocity (u_b) by using the robust *in situ* velocity observations of the annual velocity cycle at Swiss Camp to create an empirical sliding "rule" (*Anderson et al.*, 2004). The rate of change in englacial water height at a given point along the Sermeq Avannarleq flowline can be described in 1D (x) as:

$$\frac{dS}{dt} = w\varphi\frac{dh_e}{dt} = w(\dot{m}_s + \dot{m}_b) - \frac{dQ}{dx} + \dot{m}_c n_c w - \frac{dS_c}{dt} \qquad \text{Eq. 3.3.3}$$

The first term on the right is the sum of the rates of surface (m_s) and basal (m_b) meltwater input multiplied by a unit width (w; Figure 3.3.3). The second term is the horizontal divergence of water flux (dQ/dx). The third term is the meltwater generated by viscous melt inside each conduit (m_c) times the conduits per unit width ($n_c w$). The final term is the change in conduit storage volume (S_c) over time (dSc/dt). Horizontal englacial water flux variations (dQ/dx) are calculated according to non-uniform flow, whereby discharge (Q) is dependent on the englacial water height gradient (dh_e/dx; Equation 3.3.4). We may use a semi-circular conduit geometry to calculate the conduit wet cross-sectional area (A_c) and effective hydraulic diameter (D_{hc}), based on conduit radius (r), at each node.

$$Q = \sqrt{\frac{8g}{f}} \cdot A_c \cdot D_{hc}^{½} \cdot \left(\frac{dh_e}{dt}\right)^{½} \cdot n_c w \qquad \text{Eq. 3.3.4}$$

Changes in conduit storage volume (i.e. conduit size) over time (dSc/dt) occur due to: (i) the conduit volume increase due to ice volume lost by viscous melt (m_c/ρ_i), and the conduit volume change due to internal deformation. Internal deformation, which is the result of differences between ice and water overburden pressures (P_i - P_w), can either increase or decrease conduit volumes (Equation 3.3.5). The deformation term is highly non-linear, being very sensitive to both the Flow Law Parameter (A), and the Glen Number (n).

$$\frac{dS_c}{dt} = 2AS_c\left(\frac{|P_i - P_w|}{n}\right)^n - \frac{\dot{m}_c}{\rho_i} \qquad \text{Eq. 3.3.5}$$

The primary driver of this simple hydrology model is surface meltwater input (m_s). We use observed mean annual ablation rates (*Fausto et al.*, 2009), derived from GC-Net data, to prescribe the mean ablation rate along the terminal portion of the flowline. We distribute the mean ablation rate across the observed melt season with a first-order treatment, whereby the ablation rate increases linearly from zero at the onset of melt to a peak mid-season, and then decreases linearly back to zero at the cessation of melt (Figure 3.3.4).We derive an englacial entry fraction of m_s (< 1) using the ratio of ablation to accumulation at each node. To do this, we employ modeled mean annual net surface balance (*Box et al.*, 2004) and mean annual accumulation (*Burgess et al.*, 2010) rates derived from GC-Net data.

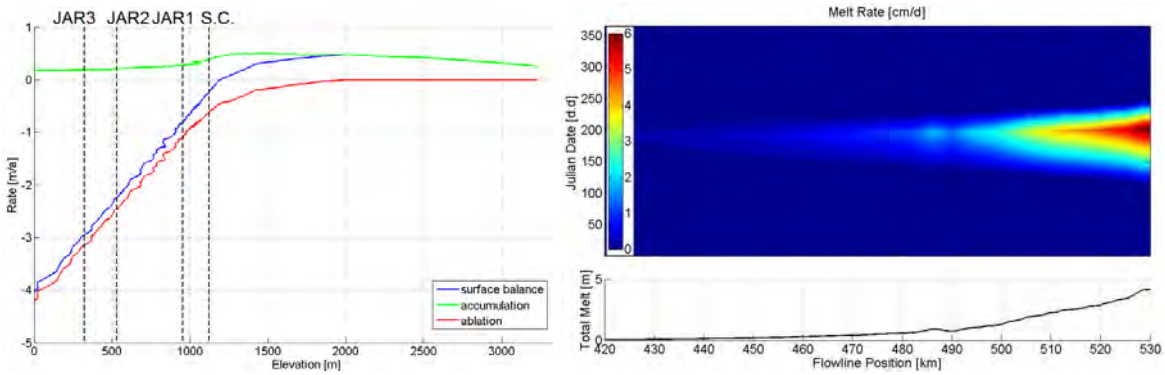

Figure 3.3.4 – Left: Annual accumulation, ablation and surface balance with elevation along the Sermeq Avannarleq flowline (Box et al., 2004; Fausto et al., 2009; Burgess et al., 2010). The AWS locations of JAR1-3 and Swiss Camp are denoted. Right: Annual observed surface ablation (melt) rate, along the terminal portion of the flowline, which drives the glaciohydrology model.

3.3.5 Ice dynamic model

The ice dynamic portion of this flowline model has been discussed at length in previous Greenland Climate Network (GC-Net) annual reports. Briefly, the ice dynamic model calculates the velocity at which the ice in the study area flows through a sophisticated solution to the vertically-integrated continuity equation:

$$\frac{dH_i}{dt} = (\dot{m}_s + \dot{m}_b) - \frac{dQ}{dx} \qquad \text{Eq. 3.3.6}$$

where the rate of change in ice thickness (dH_i/dt) at a given point along the flowline is the sum of surface (m_s) and basal (m_b) mass balance and the horizontal divergence of ice flux (dQ/dx; *Paterson*, 1994).

Important components of the flowline model are: (i) longitudinal coupling (*van der Veen*, 1987), (ii) a temperature-dependent flow law parameter (*Huybrechts et al.*, 1991), (iii) a Wisconsinan flow enhancement factor of three (*Reeh*, 1985; *Paterson*, 1991), (iv) a floating tidewater terminus with equilibrium calving flux and (v) a semi-implicit numerical method that allows time-steps of up to 25 years. At present, an estimated spatial and temporal distribution of basal sliding is used as a basal boundary condition in a ice dynamic model, until reliable basal sliding velocities are obtained from the hydrology model.

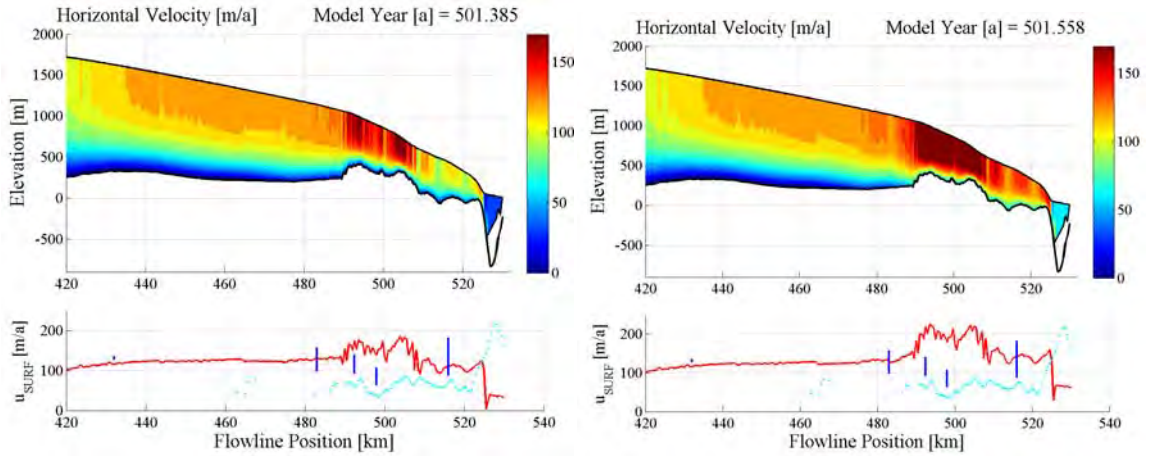

Figure 3.3.5 - Top:Ice velocities along the terminal portion of the Sermeq Avannarleq flowline. Bottom: Surface ice velocity compared to in situ GPS velocity (blue; Zwally, personal communication) and InSAR velocity (cyan; Rignot and Kanagaratnam, 2006) observations. Left to Right: Early and late melt season.

3.3.6 Preliminary results

Initializing the 1D ice dynamic model with observed Sermeq Avannarleq flowline ice topography (*Bamber et al.*, 2001; *Scambos and Haran*, 2002; *Plummer et al.*, 2008), and forcing it with observed surface mass balance (*Box et al*., 2004) results in steady-state ice velocities after a 500-year spin-up. Following spin-up, an estimated annual basal sliding cycle can be prescribed as a basal boundary condition, and the model closely reproduces *in situ* differential GPS velocity observations (Figure 3.3.5). Although modeled surface ice velocities compare reasonably well with observed *in situ* velocities, modeled surface ice velocities (as well as DGPS velocities) are consistently higher than those inferred by InSAR interferometry (*Rignot and Kanagaratnam*, 2006).

Initializing the 1D hydrology model with an "empty" Sermeq Avannarleq glacier profile and forcing it with observed ablation rates (*Fausto et al*., 2009; Figure 3.3.6) results in a steady annual englacial hydrology cycle after a 15-year spin-up. At present, subglacial conduits do not penetrate all the way from the margin to Swiss Camp. Sensitivity studies are being conducted to find the parameter space and sliding "rule" which most faithfully reproduce the observed velocity record. The relations between ice thickness (H_i) and maximum subglacial conduit radius ($r_{max}(H_i)$) and conduit spacing ($n_c(H_i)$) are the most difficult hydrological parameters to constrain through observation.

Preliminary hydrology model results suggest that the time-space dh_e/dt "fingerprint" is similar to that expected for the annual basal sliding cycle (u_b), whereby there are positive dh_e/dt values during the beginning of the melt season, when increasing u_b velocities are observed, and negative dh_e/dt values at the end of the melt season, when minimum u_b velocities occur. Therefore, it appears that basal sliding velocities are indeed proportional to the rate of change of the englacial water height (Equation 3.3.2). Thus, we have confidence in applying alpine glaciohydrology theory to this flowline of the Greenland Ice Sheet.

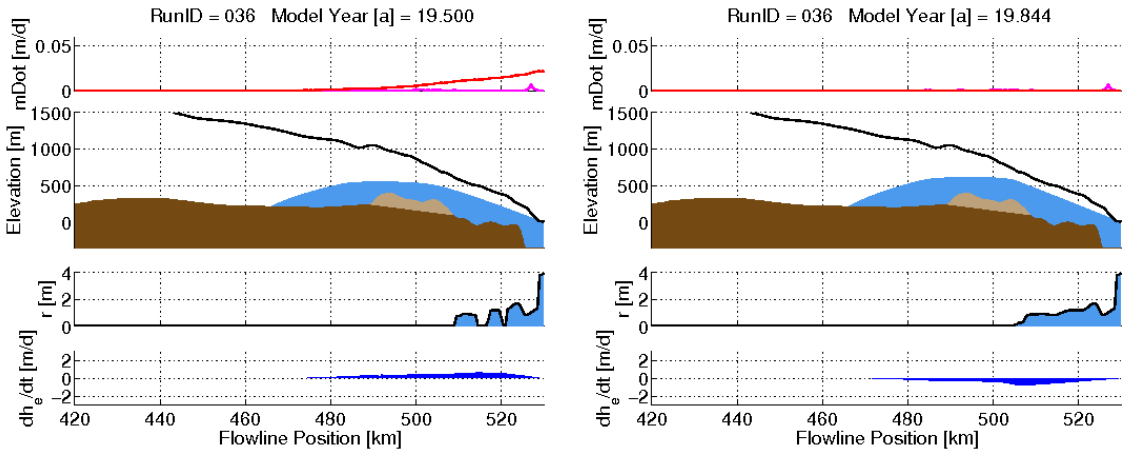

Figure 3.3.6 - The terminal portion of the Sermeq Avannarleq flowline. Top to bottom: Meltwater input due to surface (m_s; red) and basal (m_b; magenta) mass balance. Englacial water height (h_e) within the glacier using observed ice surface (black) and bedrock (brown) topography. Conduit radius (r). Rate of change in englacial water height (dh_e/dt). Left to Right: Early and late melt season.

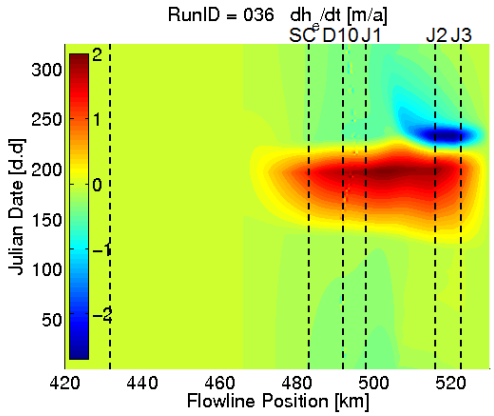

Figure 3.3.7 - Modeled time-space "fingerprint" of the rate of change of englacial water height (dh_e/dt) along the terminal portion of the Sermeq Avannarleq flowline. GC-Net AWS locations denoted with dashed lines. Conduits do not presently reach Swiss Camp (SC).

The novel aspect of using the dh_e/dt pattern to reproduce u_b values is that it reproduces the period of negative values following peak summer melt. This period of negative values is due to the model reproduction of the subglacial conduit behavior predicted by alpine glaciohydrology theory, whereby englacial water pressures increase throughout the summer melt season until they are sufficient enough to establish conduit drainage through increases in both viscous melt due to conduit discharge (driven by an increasing englacial water height gradient; dh_e/dx) and decreasing deformation closure rate (driven by decreasing effective pressure; P_i-P_w; Equation 3.3.5).

3.3.7 Outlook

This project seeks to create a physically-based glaciohydrology model to describe the temporal and spatial distribution of basal sliding of Sermeq Avannaleq flowline, in Western Greenland. Preliminary analysis of *in situ* velocity measurements from Swiss Camp yields a seasonal velocity cycle reminiscent to that expected from alpine basal sliding theory. Thus, we are confident that the application of alpine glaciohydrology theory to the Greenland Ice Sheet allows the distribution of basal sliding to be estimated under future warming scenarios. We expect a general increase in the magnitude of the annual basal sliding cycle over time, with a corresponding inland migration of the boundary to which conduits penetrate. We speculate that the magnitude of basal sliding and the duration of the sliding season are both sensitive to distance inland from the margin. Thus, we expect small

changes in the boundary of the onset of basal sliding or the duration of the sliding season to result in non-linear changes in annual total ice discharge to the ice sheet margin.

Describing the relation between surface meltwater production and basal sliding, as well as quantifying the temporal and spatial distribution of basal sliding variability, are pressing objectives for three main reasons: (i) to establish whether a non-linear relation between meltwater input and basal sliding exists, (ii) to reduce uncertainties in satellite-derived InSAR mass-balance estimates due to intra-annual basal sliding variations, and (ii) to reduce uncertainties in the projected dynamic contribution of the Greenland Ice Sheet to sea level rise due to inter-annual basal sliding variations. The theoretical and modelling advances of this project will also be applicable to assessing stability of other ice sheets and glaciers.

3.4 Moulin Basin Summer Water Budget

3.4.1 Introduction

The Greenland Ice Sheet is losing ~200 Gt yr^{-1} through increased surface meltwater runoff and enhanced outlet glacier flow (*van den Broeke et al.,* 2009; *Velicogna,* 2009; *Hanna et al.,* 2008). Recent observations find a relationship between meltwater production and accelerated glacier flow in the ablation zone (*Zwally et al.,* 2002; *van de Wal et al.,* 2008; *Shepherd et al.,* 2009). These studies hypothesize that meltwater produced at the surface rapidly drains to the ice-bedrock interface through moulins and englacial conduits. Recent observations find vertical uplift (jacking) and horizontal accelerations (50-100%) approximately 2 hrs after peak surface ablation, suggesting a very rapid transfer of water through 1 km of ice (*Shepherd et al.,* 2009). Diurnal velocity increases are manifested as a seasonal speed-up, observed using InSAR (*Joughin et al.,* 2008) although these changes do not appear to have a long-term effect on ice sheet velocity (*van de Wal et al*., 2008).

A key component in the coupling of meltwater production to enhanced glacier flow are observations of supraglacial stream discharge and the spatial distribution of meltwater input to the ice. Previous studies on the GrIS rely on modeled meltwater production through positive degree-day modeling as the input term (*Reeh,* 1991; *Braithwaite,* 1995) with limited in situ stream discharge or spatial distribution of meltwater input. A necessary step forward then is to examine the quantity of water (as a percentage of total meltwater production), the temporal lag between meltwater production and drainage and the spatial distribution of the input.

3.4.2 Methods

The site of this investigation is a small supraglacial stream basin in the ablation zone of the western flank of the Greenland Ice Sheet (Figure 3.4.1). The supraglacial hydrology network of this basin is dendritic, with multiple tributaries collecting into a single large stream that discharges into a moulin located at 69.554 °N and 49.899 °W and 776 m elevation. Panchromatic WorldView-1 imagery (50 cm horizontal resolution) was acquired of the study site 15 July 2009. Manual identification of supraglacial tributaries was used to delineate the extent of the basin, which was found to have an area (A) of 1.14 km^2.

A river gauging station was deployed on the main supraglacial stream ~ 30 m upstream from the moulin between 3 and 20 August 2009 (Julian Dates 215 to 232). During this period of the late melt season the surface of the basin consisted of hummocky ice. The river gauging station recorded water surface height with a Campbell Scientific SR-50 gauge and stream velocity with a Geopacks MFP51 Flowmeter. An automatic weather station was also deployed ~ 160 m from the gauging station. The automatic weather station recorded ice surface height using a Campbell Scientific SR50

sonic sensor, air temperature and relative humidity using a Vaisala HMP50, wind speed and direction using a RM Young 050103 wind sensor and barometric pressure using a Vaisala PTB110. An Extreme Ice Survey time-lapse digital camera (Nikon D200, 20 mm lens) was installed ~ 15 m downstream of the gauging station and recorded photographs every 15 minutes. These *in situ* observational instruments allow us to investigate the water budget of this small supraglacial basin.

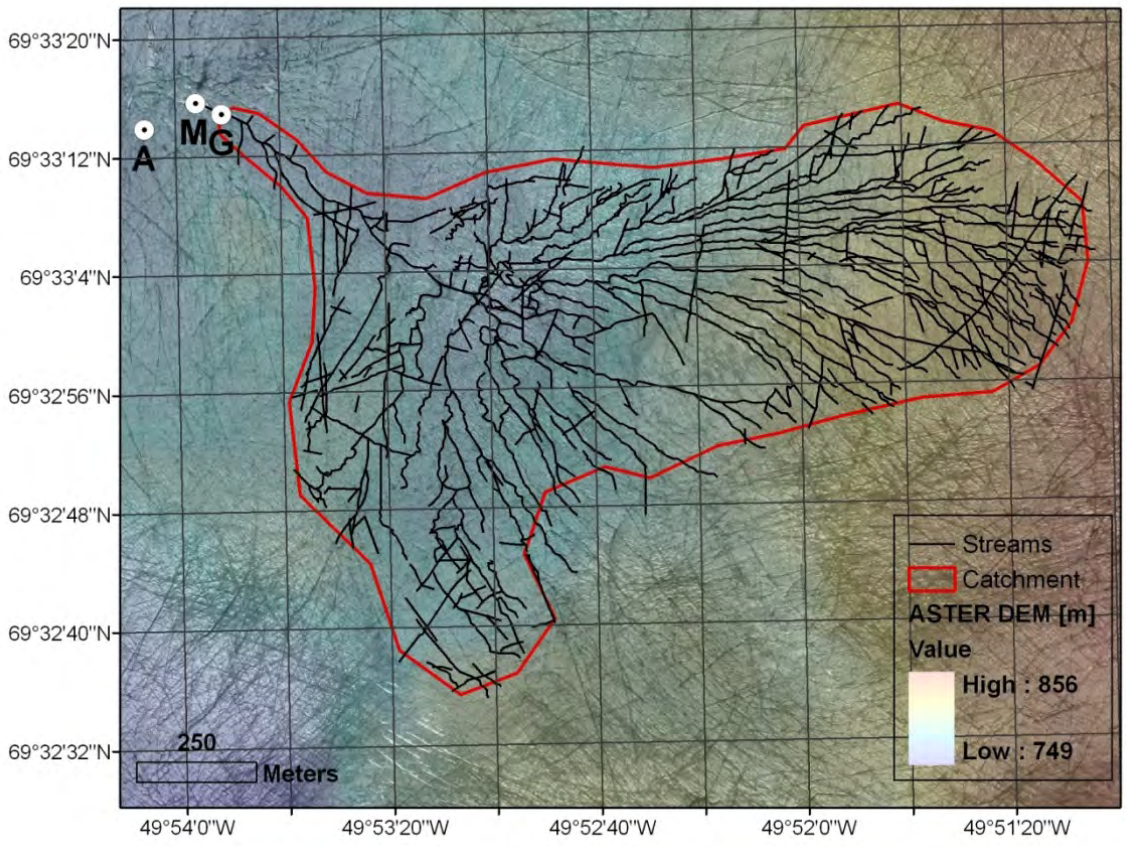

Figure 3.4.1. Moulin basin delineated on Worldview-1 Imagery. G is gauging station location, M is moulin location and A is AWS location.

Assuming conservation of water, we may formulate our basin scale water budget as a simple balance of inputs and outputs:

$$0 = (I_{MELT} + I_{RAIN}) - (Q_{MOULIN} + Q_{CREVASSE} + E) + \Delta S \qquad \text{Eq. 3.4.1}$$

where I_{MELT} and I_{RAIN} are water inputs to the basin due to ablation and rainfall, and Q_{MOULIN}, $Q_{CREVASSE}$ and E are water outputs from the basin due to moulin point discharge, crevasse distributed discharge and evaporation. The absence of supraglacial meltwater ponds within the study area suggests there cannot be a significant change in surface water storage over the study period ($\Delta S \approx 0$). Field data may be used to constrain all water budget terms except $Q_{CREVASSES}$. We treat this term as a free parameter (unknown) when solving the water budget. Thus, we may reformulate the basin scale water budget as

$$Q_{CREVASSE} = (I_{MELT} + I_{RAIN}) - (Q_{MOULIN} + E) \qquad \text{Eq. 3.4.2}$$

Meltwater input due to ablation was calculated using a positive degree-day (PDD) model. Positive degree-day modeling is a simplification of complex energy balance processes, whereby the sum of positive temperatures over a given time interval is assumed to be proportional to the cumulative ablation over that time interval (*Reeh*, 1991; *Braithwaite*, 1995). Cumulative modeled ablation was found to agree best with cumulative observed surface height change over the study period with a degree-day factor of 8.3 mmWE PDD^{-1}. This value compares well with the degree-day factor of 9.0 mm PDD^{-1} (or 8.25 mmWE PDD^{-1}) validated by Thomas et al. (2003) with *in situ* weather station data at nearby JAR2 (~17 km SSW at 570 m elevation).

Although the moulin weather station was not equipped to record liquid precipitation, we estimate water input due to rainfall from the *in situ* Extreme Ice Survey photographic record. The photographic record indicates that only two brief rainfall events occurred over the 15-day study period. The first rainfall event, 1.2 hours in duration, occurred on 3 August 2009 while the second rainfall event, 4.3 hours in duration, occurred on 11 August 2009. Both these rain events fit the description of being "light" in intensity (< 2.5 mm hr^{-1}; American Meteorological Society, 2010). We estimate the intensity (R) of the events as 0.5 ± 0.25 and 1.0 ± 0.5 mm hr^{-1} respectively.

Water output due to moulin discharge was determined from gauge station data. Unlike terrestrial river gauging where the bed is assumed to be constant over short time-scales, in supraglacial stream gauging the bed is incising into the ice at an appreciable rate. Thus, both the water surface and bed elevations vary relative to the fixed impeller elevation through time. The cross-sectional profile of the supraglacial channel was measured upon installation. We then assumed the channel geometry incised into the ice surface at a constant rate of -3.2 cm day^{-1}. This rate of incision was calculated as the mean 15-day rate of decrease in water surface height. The photographic record and measurements upon gauging station removal suggest that the assumption of constant geometry incising downward is justified. Knowing the water bed elevation, water surface elevation and cross-sectional profile allows the cross-sectional area of the stream (A_{CROSS}) to be determined at any time-step via numerical integration (dx = 2 cm).

Assuming laminar flow, depth-averaged velocity occurs at 0.42 water column height (H). A site-specific rating curve was developed using velocity values (n = 88) when the impeller was located at 0.42 ± 0.03 of water column height. These depth-averaged velocity values (u) were multiplied by the cross-sectional stream area to determine the moulin discharge. As these depth-averaged velocity values span multiple days, during which the stream bottom was incising downward, the impeller was at 0.42 H during periods of both peak and base flow. Thus, we regard our record of depth-averaged velocities as robust, in that it is not biased towards periods of high or low flow. As only one stream flowmeter was available *in situ*, we must assume there is minimal across-channel velocity variation. Given the relative wide (~ 2.5 m) and shallow (~ 0.5 m) dimensions of the stream, this is likely a valid assumption. For periods when the impeller was not located at 0.42 ± 0.03 H, discharge was calculated from a site-specific rating curve ($Q_{MOULIN} = 1.29H^2 - 0.32H$; r^2 = 0.99; Figure 3.4.2).

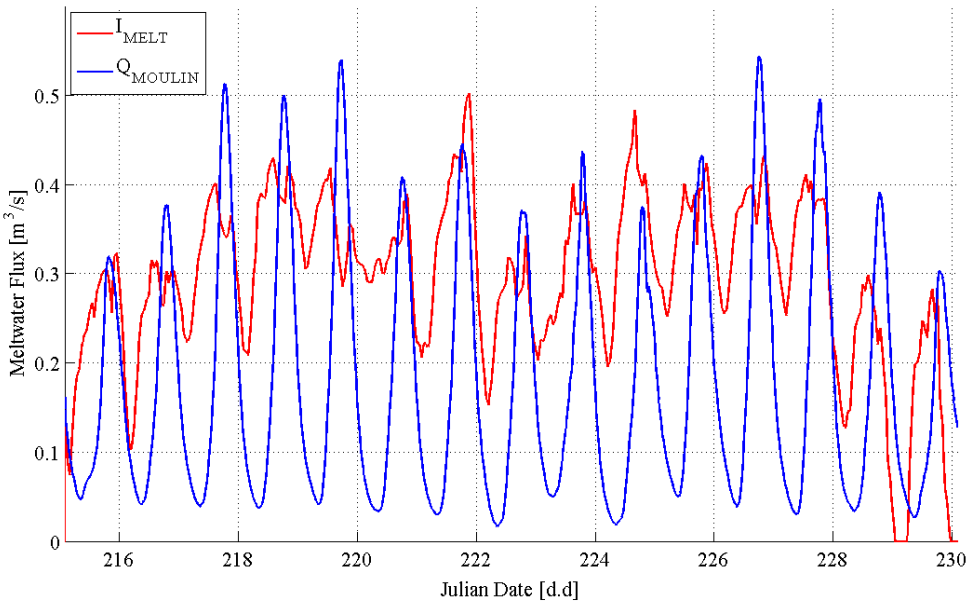

Figure 3.4.2. Instantaneous meltwater production and moulin discharge. A theoretical rate of water output due to evaporation was calculated based on latent heat flux:

$$E = Q_E / L * p_w \qquad \text{Eq. 3.4.3}$$

We assume a latent heat flux (Q_E) of 6.8 W m^{-2}, which has been observed during the month of August at the nearby JAR2 automatic weather station (~17 km SSW at 570 m elevation; *Box and Steffen*, 2001). The latent heat of sublimation (L) and density of water (ρ_w) are taken as $2.834 \cdot 10^6$ J kg^{-1} and 1000 kg m^{-3} respectively (*Box and Steffen*, 2001).

3.4.3 Results

The mean rate of meltwater input due to ablation was 2.46 x 10^4 WE m^3 day^{-1} over the 15-day study period (Figure 3.4.5). In comparison, the mean rate of water input due to rainfall was 681 WE m^3 day^{-1} over the study period. Thus, the total water input due to rainfall (0.3 %) is negligible in comparison to the water input due to ablation (99.7 %). Moulin drainage, which occurred at a mean rate of -1.51 x 10^4 WE m^3 day^{-1} over the study period, is the dominant water output term, comprising 62 % of water output from the basin. In comparison, crevasse drainage comprised 37 % (9.2 x 10^3 WE m^3 day^{-1}) of water output from the basin. Water output due to evaporation was negligible, with only 1 % (2675 WE m^3 day^{-1}) of water leaving the basin via evaporation. Although crevasse drainage is an inherently negative term, on the last day of the study period, observed moulin discharge exceeded meltwater production, resulting in a positive crevasse drainage value. This positive value, however, is within error of zero.

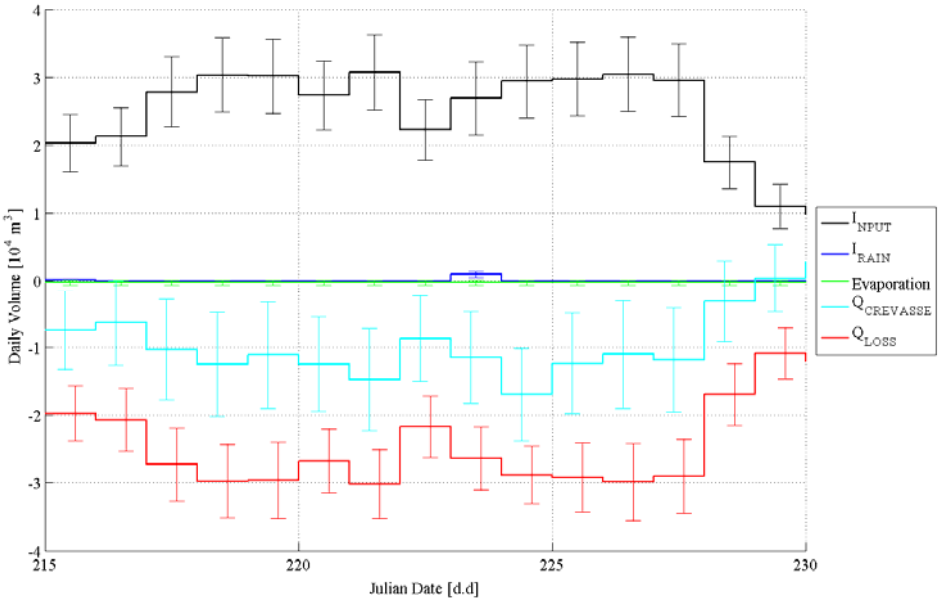

Figure 3.4.3. Daily volume of water budget components.

3.4.5 Discussion

Over 60% of meltwater produced in the basin enters the englacial system rapidly at the main moulin with mean peak discharge occurring at 15:45 (local). The discharge peak only lags mean peak meltwater production by 3.5 hrs implying a very rapid transfer of meltwater from the surface to the englacial hydrologic system. The study period occurred late in the melt season, where it is reasonable to assume that the englacial and basal hydrologic systems have sufficiently evolved to drain meltwater. Thus, the large diurnal cycle in moulin drainage would result in the englacial and basal conduits cycling between open-channel flow for most of the diurnal cycle and a pressurized channel configuration during peak discharge. *Shepherd et al.* (2009), working in a similar region of the GrIS in the late melt season, observe peak (1-4 cm) vertical uplift and horizontal displacement ~2 hrs after peak modeled meltwater production and hypothesize that this signifies that the subglacial system had become pressurized. However this result represents a discrepancy with our observed 3.5 hr lag between peak meltwater production and moulin discharge. This provides further evidence that the englacial transfer of meltwater is very rapid, even through 500-1000 m thick ice.

Diurnal and seasonal variations in meltwater input have been implicated in observed speedups along the western margin of the GrIS. *Zwally et al.* (2002) observed 5 to 28% seasonal increases in ice velocity near Swiss Camp that was correlated with seasonal meltwater production. The seasonal acceleration is most significant (~50%) along the broad regions of the western margin that are land terminating while less significant (~10-15%) for outlet glaciers, whose velocity is more directly related to changes in backstress at the calving front (*Joughin et al.*, 2008). Importantly, it seems that while the ice velocities in the ablation zone respond quickly to changes in meltwater input, over longer time scales, the internal drainage system evolves to effectively drain the increased input (*van de Wal et al.*, 2008). Observations of alpine glaciers support the hypothesis that englacial and basal conduits respond to the transient water supply, which varies on diurnal and seasonal time scales. When the input exceeds output, storage occurs at the bed surface, most likely in linked cavities peripherally located to conduits (*Harper et al.*, 2004; *Bartholomaus et al.*, 2008). Water pressure increases as input continues, leading to jacking, a reduction in the effective pressure at the bed inter-

face and finally, an increase in basal sliding (*Bartholomaus et al*., 2008). Conduit size can increase in response to this forcing through frictional melting or, as is most likely the case for the diurnal cycle, the water input decreases, allowing the linked cavities to drain, increasing the effective pressure and reducing basal motion (*Bartholomaus et al.*, 2008). GPS measurements along the western margin of the GrIS fit this hypothesis with uplift (jacking) and acceleration following peak meltwater input in the late afternoon, followed by a surface lowering and subsequent slowdown, presumably as the linked cavities drain and the basal sliding subsides (*Shepherd et al.*, 2009).

While 60% of meltwater is transferred rapidly into the englacial system, the remaining 40% either flows into crevasses or other small moulins within the basin. The paucity of melt ponds within this basin suggests that this water is drained or that there is sufficient englacial storage to account for this volume. However, the input of this water is distributed across a much greater surface area and thus the meltwater volume per crevasse/moulin is significantly smaller. This reduced volume coupled with a potentially intermittent input source (due to ice movement/deformation) would likely result in a more transient and less efficient drainage system, resulting in a longer transfer time than the main moulin system.

Previous studies have correlated meltwater production from a PDD model with diurnal and seasonal variations in ice velocity (*Zwally et al.*, 2002; *Shepherd et al.*, 2009). This correlation is based on the assumption that meltwater input to the bed increases linearly with meltwater production. Our observations of mean daily meltwater production are linearly correlated with moulin drainage, supporting this assumption (Figure 3.4.6; Q=0.26*MPDD + 0.1; r^2=0.56).

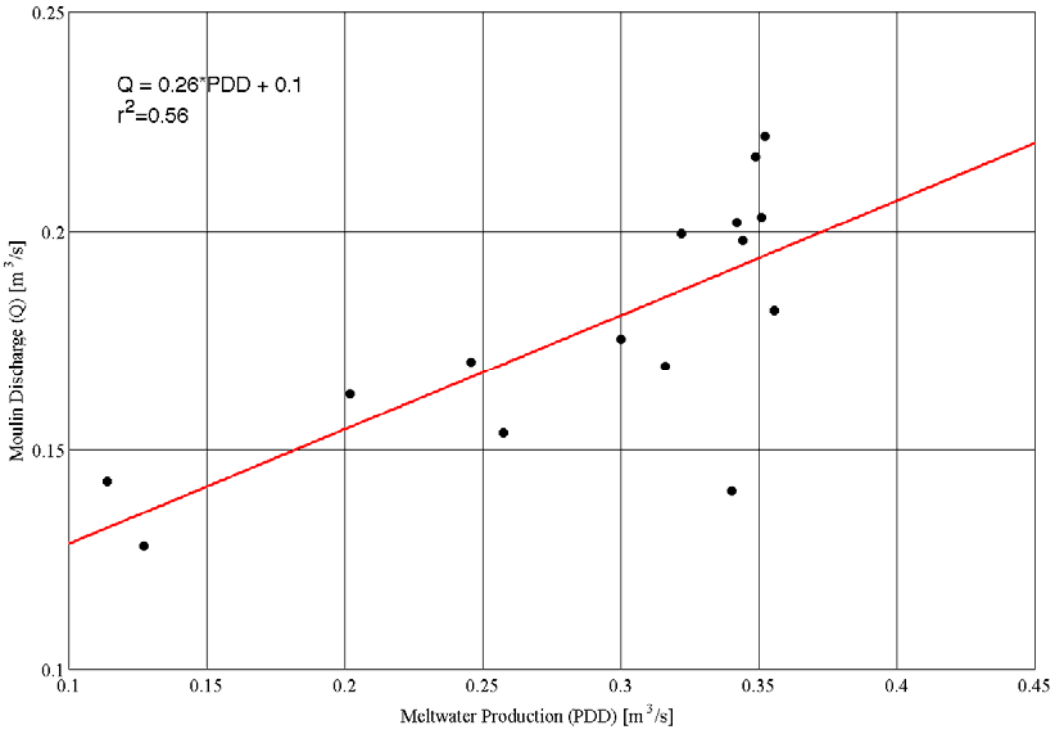

Figure 3.4.4. Moulin discharge (Q) as a function of meltwater production (PDD).

3.4.6 Conclusion

A comprehensive water budget is presented for a 1.14 km^2 basin on the western margin of the

Greenland Ice Sheet for a 15-day period during August 2009. Meltwater production was the dominant input term and was calculated using a PDD model with an 8.1 mm WE day^{-1} degree day factor. Mean meltwater input was 2.46 x 10^4 WE m^3 day^{-1} of which 1.51 x 10^4 WE m^3 day^{-1} was drained via the primary moulin in the basin, accounting for 62% of the loss. Crevasse drainage, a free term in the water budget, accounted for 37% of the loss. Rainfall and evaporation were negligible terms in the water budget. Meltwater input to the ice sheet via the moulin had a distinct diurnal cycle, peaking at 15:45 local, 3.5 hrs after peak meltwater production. The dominant diurnal cycle in meltwater input will likely cycle englacial and basal conduits between extended periods of open channel flow and brief periods of pressurized channel configuration, with important implications for basal water pressure and basal sliding. Future work will focus on constraining ice velocity and uplift coincident with supraglacial stream discharge measurements.

4. Proposed Field Activities and Research Objectives 2010

4.1 AWS Maintenance

The automatic weather station network will be maintained and upgraded. In the north, (GITS, Humboldt, Tunu-N, Petermann ELA, and NASA-SE new dataloggers (Campbell CR1000) will be installed. The new aws at the UJS/EU drilling site (NEEM) will be maintained, and we plan to visit Summit and NGRIP In the southern part of the ice sheet we will service the DYE-2, Saddle, NASA SE, Saddle, and S-Dome (Fig. 1.1), download the data and collect snow stratigraphy information. The profile JAR2, JAR1, CU/ETH, and Crawford 1 will be serviced while at the Swiss Camp.

The field season 2010 will concentrate to upgrade AWS's on the Greenland ice sheet with updated data loggers and some new instrumentation. Further, we will install new GPS unites for those AWS's that transmit via GOES satellite and need a very accurate time stamp. Several AWS's have melted out in the ablation region near Swiss Camp and need to be re-drilled.

4.2 GPS Network Maintenance

Our effort to monitor the ablation along a transect from the Swiss Camp to the ice margin will continue. We will service the GPS network in collaboration with Dr. Jay Zwally (NASA-GSFC); in collaboration with Dr. Jose Rial (Duke University), we will install a seismic network at our main moulin location. We will continue to collect high-resolution surface topography data using Trimble Pathfinder differential GPS measurements along several transects in the lower ablation region. In addition, we will acquire ICEBRIDGE laser altimeter data to derive e a high resolution elevation model for the Jakobshavn ablation region in the vicinity of our AWS's.

4.3 Ground Penetration Radar

We have collected a number of ground penetrating radar (GPR) profiles along the western slope of the ice sheet (Jakobshavn and Kangerlussuaq region) in previous field seasons (1999, 2000, 2003, and 2007, 2008). The analysis of this data set showed that the accumulation could vary up to 40% between the trough and the ridge of the undulation. The surface topography with scale length of several kilometers plays an important role for the spatial variability of accumulation, the mass transfer, and the surface energy balance. We will repeat some of these GPR measurements during the spring 2010 field season along the same profiles to verify the recent accumulation changes and high percolation events in that region. We also purchased a new MALA 10 KHz ground penetrating antenna to map the underside of the Greenland ice sheet below Swiss Camp towards the ice margin in view of our moulin modeling. We will try to assess the sub glacial conduit density and the occurrence frequency of moulin (relics) in spring 2010.

5. Bibliography

Abdalati, W. and K. Steffen, 2001. Greenland ice sheet melt extent: 1979-1999, *J. Geophys. Res.*, 106(D24), 33,983-33,989.

Anderson, R., S. Anderson, K. MacGregor, E. Waddington, S. O'Neel, C. Riihimaki and M. Loso. 2004. Strong feedbacks between hydrology and sliding of a small alpine glacier. *J. Geophys. Res.* **109** (F03005), doi:10.1029/2004JF000120.

Arnold, N. and M. Sharp. 2002. Flow variability in the Scandinavian ice sheet: modelling the coupling between ice sheet flow and hydrology. *Quaternary Science Reviews.* **21**: 485-502.

Badino, G. 2002a. Glacial karst phenomenology. La Venta, 28.

Badino, G. 2002b. Phenomenology and first numerical simulations of the freatic drainage network inside glaciers. *La Venta* 23-24, 225.

Badino, G. and L. Piccini. 2002. En-glacial water fluctuation in moulins: an example from Tyndall glacier (Patagonia, Chile). *Nimbus* 23-24, 125129.

Bamber, J., S. Ekholm and W. Krabill. 2001. A new, high-resolution digital elevation model of Greenland fully validated with airborne laser altimeter data. *J. Geophys. Res.* **106:** 6733-6745.

Bartholomaus, T., R. Anderson and S. Anderson. 2008. Response of glacier basal motion to transient water storage. *Nat. Geosci*. **1**: 33-37.

Bartholomew, I., P. Nienow, D. Mair, A. Hubbard, M. King and A. Sole. *in press*. Seasonal evolution of subglacial drainage and acceleration in a Greenland outlet glacier. *Nat. Geosci.*

Box, J., D. Bromwich and L. Bai. 2004. Greenland ice sheet surface mass balance 1991-2000: Application of Polar MM5 mesoscale model and in situ data. *J. Geophys. Res.* **109** (D16105), doi:10.1029/2003JD004451.

Box, J., K. Steffen . 2001. Sublimation on the Greenland ice sheet from automated weather station observations. *J. Geophys. Res.* **106**(D24): 33,965-33,981.

Braithwaite, R. J. 1995. Positive degree-day factors for ablation on the Greenland ice sheet studied by energy balance modelling. *J. Glaciology* **41**(137): 153-160.

Budd, W. F . 1969. The dynamics of ice masses. AN ARE Scientific Reports, Publ. No. 108. 212 pp.

Burgess, E., R. Forster, J. Box, E. Mosley-Thompson, D. Bromwich, R. Bales and L. Smith. 2010. A spatially calibrated model of annual accumulation rate on the Greenland Ice Sheet (1958-2007). *J. Geophys. Res.* **115** (F02004), doi:10.1029/2009JF001293.

Corne S., Murray T., Openshaw S., See L., and Turton I., 1999. Using computational intelligence techniques to model subglacial water systems. *J. Geogr. Sys.*, 1, 37-60.

Duval, P and H. LeGac. 1977. The role of the water content on the creep rate of polycrystalline ice. *IAHS*, 118, 29-33.

Fausto, R., A. Alstrom, D. van As, C. Boggild and S. Johnsen. 2009. A new present-day temperature parameterization for Greenland. *J. Glaciol*. **55**: 95-105.

Fountain, A. and J. Walder. 1998. Water Flow through Temperate Glaciers. *Rev. Geophys.* **36**: 299-328.

Funk, M., K. Echelmeyer and A. Iken. 1994. Mechanisms of fast flow in Jakobshavn Isbrae, West Greenland: Part II Modeling of englacial temperatures, *Journal of Glaciology* 40(136), 569-585.

Hanna, E., P. Huybrechts, K. Steffen, J. Cappelen, R. Huff, C. Shuman, T. Irvine-Fynn, S. Wise, M. Griffiths. 2008. Increased Runoff from Melt from the Greenland Ice Sheet: A Response to Global Warming. *J. Climate* **21**: 331-341.

Hanna, E., R. Huybrechts, I. Janssens, J. Cappelen, K. Steffen and A. Stephens. 2005. Runoff and mass balance of the Greenland ice sheet: 1958-2003. *J. Geophys. Res.* **110** (B13108), doi:10.1029/2004JD005641.

Harper, J., N. Humphrey, W.T. Pfeffer, B. Lazar. 2007. Two modes of accelerated glacier sliding related to water. *Geophysical Research Letters* **34**.

Hooke, R. L. 2000. Principles of Glacier Mechanics, Cambridge University Press.

Hooke R. LeB. 1976. Pleistocene Ice at the Base of the Barens Ice Cap, Baffin Island, N.W.T., Canada, *Journal of Glaciology*, 17(75), 49-59.

Joughin, I., S. Das, M. King, B. Smith, I. Howat, T. Moon. 2009. Seasonal Speedup Along the Western Flank of the Greenland Ice Sheet. *Science* **320**.

Huybrechts, P., A. Letreguilly and N. Reeh. 1991. The Greenland ice sheet and greenhouse warming. *Glob. Plan. Chg.* **3**: 399-412.

Joughin, I., S. Das, M. King, B. Smith, I. Howat and T. Moon. 2008. Seasonal speedup along the western flank of the Greenland Ice Sheet. *Science*. **320**: 781-783.

Murray, T. & Clarke, G. K. C. 1995, Black-box modeling of the subglacial water system. *Journal of Geophysical Research*, 100(B7), 10219-10230.

Nghiem, S.V., K. Steffen, R. Kwok, and W.Y. Tsai. 2001. Diurnal variations of melt regions on the Greenland ice sheet, *J. Glaciol.*, 47(159), 539-547.

Kamb, B., H. Engelhardt, M. Fahnestock and N. Humphrey. 1994. Mechanical and hydrologic basis for the rapid motion of a large tidewater glacier 2. Interpretation. *J. Geophys. Res.* **99**:

Marshall, S. 2005. Recent advances in understanding ice sheet dynamics. *Earth Plan. Sci. Lett.* **204**: 191-204.

Paterson, W. 1991. Why ice-age ice is sometimes “soft”. *Cold Reg. Sci. Tech.* **20**: 75-98.

Paterson, W. 1994. The Physics of Glaciers. Oxford, England: Butterworth-Heinemann.

Plummer, J., S. Gogineni, C. van der Veen, C. Leuschen and J. Li. 2008. Ice Thickness and bed map for Jakobshavn Isbrae, CReSIS Tech Report #2008-1.

Reeh, N. 1985. Was the Greenland ice sheet thinner in the late Wisconsinan than now? *Nature*. **317**: 797-799.

Reeh, N. 1991. Parameterization of melt rate and surface temperature on the Greenland ice sheet. *Polarforschung* **59**(3): 113-128.

Rignot, E. and P. Kanagaratnam. 2006. Changes in the Velocity Structure of the Greenland Ice Sheet. *Science.* **311**: 986-990.

Scambos, T. and T. Haran. 2002. An image-enhanced DEM of the Greenland ice sheet. 2002. *Ann. Glaciol.* **34**: 291-298.

Thomas, R., W. Abdalati, E. Frederick, W. Krabill, S. Manizade, K. Steffen 2003. Investigation of

surface melting and dynamic thinning on Jakobshavn Isbræ, Greenland. *J. Glaciology* **49**(165): 231-239.

van de Wal, R. S. W., W. Boot, M. van den Broeke, C. Smeets, R. Reijmer, J. Donker, J. Oerlemans 2008. Large and Rapid Melt-Induced Velocity Changes in the Ablation Zone of the Greenland Ice Sheet. *Science* **321**(111).

van den Broeke, M., J. Bamber, et al. 2009. Partitioning Recent Greenland Mass Loss. *Science* **326**(5955): 984-986.

van der Veen, C. 1987. Dynamics of the West Antarctic Ice Sheet. ed. C. van der Veen and J. Oerlemans.

Velicogna, I. 2009. Increasing rates of ice mass loss from the Greenland and Antarctic ice sheets revealed by GRACE. *Geophysical Research Lettters* **36**.

Zwally, H., W. Abdalati, T. Herring, K. Larson, J. Saba and K. Steffen. 2002. Surface melt-induced acceleration of Greenland Ice Sheet flow. *Science.* **297**: 218-222.